OTÁVIO RIZZI COELHO FILHO

CARACTERIZAÇÃO CONJUNTA DA FIBROSE INTERSTICIAL E DA HIPERTROFIA DOS CARDIOMIÓCITOS PELA RESSONÂNCIA MAGNÉTICA CARDÍACA

"CHARACTERIZATION OF BOTH INTERSTITIAL FIBROSIS AND CARDIOMYOCYTE HYPERTROPHY BY CARDIAC MAGNETIC RESONANCE"

CAMPINAS

2013

Universidade Estadual de Campinas

Faculdade de Ciências Médicas

OTÁVIO RIZZI COELHO FILHO

CARACTERIZAÇÃO CONJUNTA DA FIBROSE INTERSTICIAL E DA HIPERTROFIA DOS CARDIOMIÓCITOS PELA RESSONÂNCIA MAGNÉTICA CARDÍACA

"CHARACTERIZATION OF BOTH INTERSTITIAL FIBROSIS AND CARDIOMYOCYTE HYPERTROPHY BY CARDIAC MAGNETIC RESONANCE"

Orientador: Prof. Dr Wilson Nadruz Júnior

Tese de Doutorado apresentada à Comissão de Pós-Graduação em Clínica Médica da Faculdade de Ciências Médicas da Universidade Estadual de Campinas para obtenção do título de Doutor em Clínica Médica, área de concentração Clínica Médica

Doctoral Thesis presented to the Internal Medicine Postgraduate Program of the Faculty of Medical Sciences, State University of Campinas, for obtainment of the Ph.D. degree in Internal Medicine, specialization in Internal Medicine

Este exemplar corresponde à versão final da tese de doutorado defendida pelo aluno **OTÁVIO RIZZI COELHO FILHO** e orientada pelo **PROF. DR. WILSON NADRUZ JÚNIOR**

_____

Assinatura do Orientador

CAMPINAS
2013

Ficha catalográfica
Universidade Estadual de Campinas
Biblioteca da Faculdade de Ciências Médicas
Maristella Soares dos Santos - CRB 8/8402

C65c

Coelho Filho, Otávio Rizzi, 1977-
Caracterização conjunta da fibrose intersticial e da hipertrofia dos cardiomiócitos pela ressonância magnética cardíaca / Otávio Rizzi Ceolho Filho. – Campinas, SP : [s.n.], 2013.

Orientador: Wilson Nadruz Junior.
Tese (doutorado) – Universidade Estadual de Campinas, Faculdade de Ciências Médicas.

1. Ressonância magnética. 2. Fibrose miocárdica. 3. Hipertrofia. 4. Hipertensão. 5. Gadolínio. I. Nadruz Junior, Wilson,1973-. II. Universidade Estadual de Campinas. Faculdade de Ciências Médicas. III. Título.

Informações para Biblioteca Digital

Título em inglês: Characterization of both interstitial fibrosis and cardiomyocyte hypertrophy by cardiac magnetic ressonance
Palavras-chave em inglês:
Magnetic ressonance
Myocardial fibrosis
Hypertension
Hypertrophy
Gadolinium
Área de concentração: Clínica Médica
Titulação: Doutor em Clínica Médica
Banca examinadora:
Wilson Nadruz Junior [Orientador]
Lício Augusto Velloso
Li Li Min
José Rodrigues Parga Filho
André Schmidt
Data de defesa: 10-06-2013
Programa de Pós-Graduação: Clínica Médica

BANCA EXAMINADORA DA DEFESA DE DOUTORADO

OTÁVIO RIZZI COELHO FILHO

Orientador (a) PROF(A). DR(A). WILSON NADRUZ JUNIOR

MEMBROS:

1. **PROF(A). DR(A). WILSON NADRUZ JÚNIOR** _____
2. **PROF(A). DR(A). LÍCIO AUGUSTO VELLOSO** _____
3. **PROF(A). DR(A). LI LI MIN** _____
4. **PROF(A).DR(A). JOSÉ RODRIGUES PARGA FILHO** _____
5. **PROF(A).DR(A). ANDRÉ SCHMIDT** _____

Programa de Pós-Graduação em Clínica Médica da Faculdade de Ciências Médicas da Universidade Estadual de Campinas

Data: 10 de junho de 2013

Dedico este trabalho...

Ao meu pai, minha mãe, minha irmã e minha esposa,
pelo incansável suporte...

AGRADECIMENTOS

Agradeço ao meu pai Otavio Rizzi Coelho, exemplo maior de profissional ético, médico, amigo, professor e líder. Tenho o privilégio de contar com seu apoio desde os meus primeiros momentos de vida.

Agradeço ao querido Professor Michael Jerosch-Herold, um exemplo impecável de cientista e mentor. Sua dedicação, disposição, generosidade e incansáveis ensinamentos formam os alicerces desse projeto. Nosso convívio me instruiu muito mais do que eu poderia imaginar além de me coroar com a sua amizade.

Agradeço ao colega Ravi Shah, pelo constante incentivo, apoio e dedicação.

Agradeço ao meu orientador Prof. Wilson Nadruz Júnior, pela cuidadosa e dedicada orientação.

Agradeço à minha família.

Agradeço à minha esposa.

“Nem tudo que se enfrenta pode ser modificado,
mas nada pode ser modificado até que seja enfrentado.”

Albert Einstein

RESUMO

A hipertrofia dos cardiomiócitos e a expansão da matriz extracelular são fatores importantes para o desenvolvimento da insuficiência cardíaca. Até o momento nenhum método não invasivo é capaz de caracterizar conjuntamente a hipertrofia de cardiomiócitos e a expansão da matriz extracelular. O objetivo desse estudo foi de validar um método derivado da ressonância magnética cardíaca (RMC) para a avaliação conjunta da hipertrofia dos cardiomiócitos e da expansão da matriz extracelular. Camundongos adultos foram submetidos a 7 semanas de tratamento com L-NG-Nitroarginine Methyl Ester (L-NAME) para indução de hipertensão e hipertrofia ventricular. Outro grupo de camundongos foi submetido à bandagem cirúrgica da aorta ascendente. Os animais tratados com L-NAME foram estudados pela RMC antes e após 7 semanas de tratamento com L-NAME. Os animais submetidos à bandagem da aorta foram estudados com 2, 4 e 7 semanas após a bandagem. O tempo T1 foi mensurado no coração antes e depois da administração de contraste paramagnético extracelular, gadolínio. O tempo de vida intracelular das moléculas de água (TVIMA), um parâmetro dependente ao tamanho da celular, e a fração do volume extracelular (FVEC), um parâmetro relacionado com o tecido conectivo extracelular, foram determinados utilizando um modelo de dois compartimentos, considerando a troca de água pela membrana celular dos cardiomiócitos. Os diâmetros menor (D_{minor}) e maior (D_{major}) dos cardiomiócitos foram medidos nos corações explantados corados com aglutinina contra gérmen de trigo (FITC-wheat germ agglutinin).

TVIMA apresentou forte correlação com a relação do volume-pela-superfície dos cardiomiócitos (r=0,78, *P*<0,001) e do volume (r=0,78, *P*<0,001) dos cardiomiócitos determinados pela histologia. Os diâmetros e o volume dos cardiomiócitos foram significativamente maior nos animais trados com L-NAME (P<0,001). Os camundongos submetidos a bandagem da aorta apresentavam sinais precoces de aumento do tamanho dos cardiomiócitos, determinado tanto pela RMC como pela histologia. Animais expostos a bandagem da aorta demonstraram aumento significante no volume e da relação volume-pela-superfície dos cardiomiócitos, assim com ocorreu com TVIMA.

A determinação do TVIMA e da FVEC pela RMC é capaz de quantificar dois importantes componentes do remodelamento cardíaco: a hipertrofia dos cardiomiócitos e a expansão da matriz extracelular.

ABSTRACT

Cardiomyocyte hypertrophy is a critical precursor to the development of heart failure. Methods to phenotype cellular hypertrophy non-invasively are limited. The goal was to validate a CMR-based approach for the combined assessment of extracellular matrix expansion and cardiomyocyte hypertrophy. Two murine models of pressure-overload, hypertension induced by L-NG-Nitroarginine Methyl Ester (L-NAME) and transaortic constriction (TAC), were imaged by CMR at baseline and 7-weeks after L-NAME treatment, and up to 7 weeks following TAC. T1 relaxation times were measured before and after gadolinium contrast. The intracellular lifetime of water (τ_{ic}), a cell size dependent parameter, and extracellular volume fraction (ECV), a parameter linked to interstitial connective tissue, were determined with a model for transcytolemmal water exchange. Minor (D_{min}) and major (D_{maj}) cell-diameters were measured on FITC-wheat germ agglutinin stained sections.

$\tau_{ic,}$ correlated strongly with histologic cardiomyocyte volume-to-surface ratio (r=0.78, P<0.001) and cell volume (r=0.75; P<0.001). Histological cardiomyocyte diameters and cell volume were higher in mice treated with L-NAME for 7 weeks compared to controls (P<0.001). In the TAC model, there was an early increase in cell volume and cardiomyocyte size using both CMR and histology without early fibrosis. Mice exposed to TAC demonstrated a significant, longitudinal, and parallel increase in histological cell volume, volume-to-surface ratio, and $\tau_{ic,}$ between 2 and 7 weeks after TAC.

The intracellular lifetime (τ_{ic}) measured by contrast-enhanced CMR is a sensitive, non-invasive measure of cardiomyocyte hypertrophy that can longitudinally track hypertrophy and myocardial remodeling.

FVEC- Fração do volume da matriz extracelular

HVE- Hipertrofia ventricular esquerda

L-NAME- L-NG-Nitroarginine Methyl Ester

RFC- Reserva do fluxo coronariano

RMC- Ressonância magnética cardíaca

RT- Realce Tardio

TVIMA- Tempo de vida intracelular das moléculas de água

LISTA DE TABELA

LISTA DE FIGURAS

SUMÁRIO

1- INTRODUÇÃO GERAL

1.1- Hipertrofia miocárdica

O músculo cardíaco é capaz de crescer em reposta a diversos estímulos. O exercício físico, a gravidez e o crescimento após o nascimento promovem o crescimento e a hipertrofia fisiológica do músculo cardíaco, enquanto que a ativação neuro-humoral, a hipertensão arterial e a lesão miocárdica causam a hipertrofia miocárdica patológica (1). A hipertrofia miocárdica patológica está associada a uma série alterações estruturais dos cardiomiócitos e de outros elementos como a matriz de estroma extracelular (2,3). Ao contrário do que ocorre na hipertrofia fisiológica, a hipertrofia ventricular esquerda (HVE) patológica está associada a um prognóstico desfavorável e ao aumento do risco para eventos cardiovasculares em geral. Por exemplo, em pacientes hipertensos, a HVE é um fator de risco independente para ocorrência de eventos cardiovasculares e de insuficiência cardíaca (3), além de morte por qualquer causa(4).

Nos últimos anos, diferentes grupos relataram que as alterações patológicas presentes na cardiopatia por hipertensão constituem mais do que o aumento da massa ventricular esquerda isoladamente (5-11). Esses dados tem dado suporte ao conceito de que a HVE é um marcador precoce, e em algumas circunstâncias, pré-clínico de doença do músculo cardíaco (12).

1.2- Definições

A hipertrofia miocárdica fisiológica pode ocorrer durante o crescimento normal dos indivíduos, durante a gravidez e em resposta a certos estímulos entre estes o exercício físico. No caso da hipertrofia fisiológica, a função cardíaca é normal e não existe associação direta com o desenvolvimento subsequente de insuficiência cardíaca (13,14). Ao contrário da hipertrofia fisiológica, a HVE patológica é causada por diversos estímulos, especialmente os biomecânicos e neuro-humorais (15). A HVE miocárdica está diretamente relacionada aos níveis de pressão arterial, apesar de outros fatores, como sexo, etnia, obesidade,

diabetes, consumo de sal e estímulos mediados pelo sistema renina-angiotensina-aldosterona e sistema nervoso simpático, também desempenham papel importante em sua gênese (14). A HVE miocárdica se caracteriza por alterações estruturais, funcionais e metabólicas do miocárdio, as quais incluem aumento no volume dos cardiomiócitos, aumento na espessura da parede das artérias coronárias, rarefação relativa de capilares, fibrose intersticial extracelular, além de modificações no metabolismo energético, na contratilidade e no relaxamento do miocárdio (16,17). Classicamente, as alterações morfológicas do ventrículo esquerdo induzidas pela hipertensão arterial podem ser divididas em três padrões geométricos principais (18,19): **1-** Remodelamento concêntrico (aumento da espessura relativa da parede ventricular com massa miocárdica normal); **2-** HVE concêntrica (aumento da espessura relativa da parede ventricular e da massa miocárdica); **3-** HVE excêntrica (aumento da massa miocárdica com elevação do volume da cavidade ventricular). A HVE concêntrica é o padrão geométrico ventricular mais associado à progressão para insuficiência cardíaca com sintomas (20). Mesmo em pacientes com massa ventricular esquerda normal, a definição da geometria do ventrículo esquerdo, em particular, o remodelamento concêntrico, é um importante marcador de risco cardiovascular (21). Embora a sobrecarga pressórica seja o principal fator determinante para o remodelamento ventricular e para a HVE, fatores como a ingestão de sal, ativação da atividade simpática, níveis de neurohormônios, fatores autócrinos e parácrinos, etilismo, obesidade, *diabetes mellitus*, exercício físico e estresse oxidativo também podem contribuir para o aumento exacerbado da massa do músculo cardíaco em pacientes hipertensos (15).

1.3- Importância clinica da hipertrofia miocárdica

O conceito de que a HVE é uma resposta adaptativa a sobrecarga hemodinâmica, podendo evoluir para disfunção ventricular é antiga. Relatos de Austin Flint, publicados em 1870 (22), descrevem claramente a relação entre

sobrecarga hemodinâmica e o aumento da massa do ventrículo esquerdo. Austin Flint ainda sugeriu que a hipertrofia do miocárdio era um fator de proteção para o desenvolvimento de dilatação e disfunção miocárdica. Alguns anos mais tarde, Willian Osler (23) evidenciou que a desadaptação ocorre frequentemente, sendo que é antecedida pela hipertrofia do músculo cardíaco.

Atualmente a HVE não é considerada apenas uma resposta compensatória incidental secundária à hipertensão arterial sistêmica, sendo reconhecida como um importante marcador de risco para doença cardiovascular. Recentes estudos populacionais indicam que cada incremento de 39g na massa ventricular esquerda por metro quadrado confere 40% de aumento no risco de ocorrência de eventos cardiovasculares (24). Observações clínicas documentaram a relação da HVE com a progressão para disfunção do músculo cardíaco e para insuficiência cardíaca. Estudos epidemiológicos observacionais com pacientes hipertensos, mostraram existir relação inversa da massa ventricular esquerda com a desempenho sistólica do músculo cardíaco, avaliada pela fração de ejeção do ventrículo esquerdo (25-27). Além disso, ensaios clínicos prospectivos evidenciaram que intervenções farmacológicas podem induzir a regressão da HVE e em paralelo melhorar os índices de desempenho sistólica do ventrículo esquerdo (28-30). O aumento da massa do músculo cardíaco também apresenta íntima associação com a disfunção diastólica do ventrículo esquerdo (30-32).

O *Framingham Heart Study* forneceu dados consistentes e inequívocos da associação da HVE com o desenvolvimento de insuficiência cardíaca (33). Nesse estudo, mais de 5 mil pacientes adultos foram seguidos por cerca de 30 anos, sendo que a presença de HVE no ecocardiograma foi um dos mais importantes fatores associados ao desenvolvimento de insuficiência cardíaca com sintomas clínicos. Os indivíduos com sinais de HVE ao eletrocardiograma de repouso apresentavam risco de apresentar insuficiência cardíaca duas a cinco vezes maior que a população saudável sem HVE. Uma interessante análise do estudo *Cardiovascular Health Study*, que seguiu mais de 2 mil pacientes sem antecedente de infarto do miocárdio e com idade avançada, forneceu evidências

que o aumento da massa do ventrículo esquerdo é um fator de risco independente para ocorrência de insuficiência cardíaca sistólica e diastólica (3).

1.4- Sobrecarga pressórica: consequências no músculo cardíaco

Um componente fundamental da resposta do cardiomiócitos ao aumento da pressão hemodinâmica a que são submetidos, é a diminuição da velocidade máxima de encurtamento, com consequente diminuição do calor produzido por grama de músculo durante contração ativa (10). Estudos de termodinâmica sugerem que esta diminuição ocorre devido ao aumento no recrutamento de cadeias de miosina. Enquanto a diminuição da velocidade máxima de encurtamento é um evento benéfico ao nível dos cardiomiócitos, permitindo que as fibras cardíacas se mobilizem a um custo energético normal; ao nível do coração como um todo, a diminuição da velocidade máxima de encurtamento é um dos primeiros fatores para o desenvolvimento da disfunção ou falência (34). Outro componente conhecido da resposta dos cardiomiócitos à sobrecarga pressórica incluiu modificações quantitativas, levando ao aumento do tamanho celular, com consequente aumento das unidades de contração (35,36).

Nas últimas duas décadas diversos estudos demonstraram que a hipertrofia dos cardiomiócitos não é a única alteração da doença cardíaca hipertensiva. Sabemos hoje, que uma série de alterações ocorrem em componentes cardíacos não musculares. As principais alterações estão representadas na Tabela 1. Um componente importante da fisiopatologia da doença cardíaca hipertensiva é a isquemia subendocárdica, induzida pelo aumento da massa ventricular esquerda e pela alteração na microcirculação coronariana, com a consequente diminuição da reserva do fluxo coronariano (37). A alteração da microcirculação é ainda agravada por alterações na funcionalidade vascular, que está frequentemente presente na hipertensão arterial, causando vasoconstrição por disfunção endotelial pela redução da produção de oxido nítrico (38). O aumento da rigidez arterial que acelera a velocidade da onda

de pulso aórtica, aumenta a pressão de esvaziamento do ventrículo esquerdo e a pressão de pulso central, diminuindo a pressão sanguínea diastólica e consequentemente a perfusão coronariana (39).

Tabela 1- Componentes fisiopatológicos do remodelamento da doença cardíaca hipertensiva

	Componentes	**Impacto fisiopatológico**
Ao nível vascular	Rarefação capilar Alterações arteriolares	Redução da RFC
Ao nível extracelular	Fibrose intersticial Fibrose perivascular	Disfunção diastólica Arritmia
Ao nível do cardiomiócito	Hipertrofia Aumento da apoptose	Redução RFC Disfunção sistólica/diastólica
Ao nível de todo órgão	Remodelamento	Dessincronia ventricular

RFC: reserva de fluxo coronariano

A deposição exagerada de fibras de colágeno tipo I e III resulta no aumento da fibrose intersticial e perivascular miocárdica (40). Por sua vez a fibrose intersticial aumenta a rigidez das paredes ventriculares, levando à disfunção diastólica (41), além da alteração dos potenciais elétricos no músculo cardíaco, o que predispõe a arritmias ventriculares (42,43). O aumento da matriz de estroma extracelular também contribui para a queda da reserva do fluxo coronariano, devido à redução da distendibilidade das paredes do ventrículo esquerdo (44). A fibrose intersticial é resultado da alteração de um complexo processo que controla o metabolismo do colágeno pelos fibroblastos e pelos miofibrolastos sob a influência de fatores pró-fibróticos (45). Estudos mais recentes sugerem também que a fibrose perivascular pode ser secundária à resposta reparadora dos fibroblastos à infiltração local de células inflamatórias e moléculas de adesão ao endotélio vascular (46).

A apoptose dos cardiomiócitos está significativamente elevada nos pacientes com cardiopatia hipertensiva (47,48), especialmente quando a insuficiência cardíaca com redução da fração de ejeção está presente (49). Evidências apontam que a apoptose pode contribuir para a perda da função contrátil do músculo cardíaco por dois mecanismos: morte celular ou por induzir alterações em organelas intracelulares envolvidas na obtenção de energia (50).

Todas as alterações descritas do remodelamento cardíaco podem causar retardo na ativação elétrica dos cardiomiócitos, que culmina com a dispersão da ativação elétrica regional do músculo cardíaco, causando distúrbios de condução e dessincroniza da despolarização ventricular (51). A dissincronia ventricular elétrica e mecânica piora a *performance* sistólica do ventrículo esquerdo, sendo também um marcador prognóstico na insuficiência cardíaca (52).

1.5- Ressonância magnética cardíaca

A técnica do realce tardio (RT) após injeção de gadolínio-DTPA pela ressonância magnética cardiovascular (RMC) se tornou o método de escolha para detecção de necrose e fibrose miocárdica com alta resolução (53,54). O realce tardio é baseado na identificação de áreas focais e densas de realce relativas a áreas normais do miocárdico. Em diversas condições clínicas, tais como na cardiopatia isquêmica, cardiopatia dilatada não isquêmica, cardiopatia diabética, cardiopatia hipertensiva e até mesmo na cardiopatia secundária ao uso quimioterápicos, a presença de fibrose foi comprovada como um marcador do remodelamento ventricular (55-59). Sabemos que o RT pode estar ausente ou apenas oferecer uma quantificação parcial da extensão do acometimento miocárdico, sendo que isto é particularmente verdade em condições em que a lesão cardíaca é difusa, como é o caso da cardiopatia hipertensiva. A presença de fibrose intersticial é um fator de risco independente para morte súbita (60) e insuficiência cardíaca (61), sendo que até a presente data nenhum método de imagem não-invasivo, incluindo o RT pela RMC, consegue detectar a fibrose intersticial de forma precisa. Mais recentemente, o Dr. Jerosch-Herold

descreveu uma técnica baseada na determinação da distribuição relativa do volume de gadolínio injetado e nas mudanças no T1 do miocárdio para quantificar o volume extracelular do miocárdio como um marcador de fibrose e remodelamento. Como o tecido fibrótico é o principal constituinte do espaço intersticial, Jerosch-Herold introduziu o termo "índice de fibrose" se referindo a fração do volume da matriz extracelular (FVEC). Foi demonstrado que através da medida do coeficiente de partição do gadolínio no miocárdio (λ_{GD}) (fórmula 1), era possível estimar precisamente o FVEC e determinar o "índice de fibrose" como um marcador objetivo de remodelamento cardíaco (62). O "índex de fibrose" é uma medida contínua e quantitativa do remodelamento extracelular, podendo ir desde o miocárdio normal, passando pelo miocárdio com fibrose intersticial, indo até fibrose difusa extensa com miocárdio não viável e cicatriz (Figura 1). O "índex de fibrose" é derivado do coeficiente de partição do gadolínio no miocárdio, corrigindo para concentração do gadolínio no sangue com a medida do hematócrito. Como o colágeno é o constituinte sólido predominante do FVEC, o valor do coeficiente de partição se correlacionou muito bem com o volume de colágeno pela biopsia cardíaca, como foi demonstrado por Flett e colaboradores (63). Dessa forma o "índice de fibrose" parece ser um marcador extremamente sensível e potencialmente precoce, com possíveis aplicações em qualquer cardiomiopatia que envolva aumento de FVEC. Mais recentemente nosso grupo demonstrou a utilidade da quantificação do FVEC pela RMC em algumas condições clínicas, como na suspeita de doença cardíaca por depósito (64) e na cardiotoxicidade pelo uso de quimioterápicos derivados da antraciclina (65). Devido aos elevados custos e aos riscos inerentes de complicação da biopsia cardíaca, a determinação da FVEC parece ser uma alternativa muito interessante e não-invasiva para quantificação do grau de remodelamento cardíaco. Além disso, até o momento, a avaliação não-invasiva da doença cardíaca hipertensiva se restringiu apenas a uma avaliação morfológica e funcional , sendo que não resta dúvidas que as alterações morfológicas e funcionais são eventos tardios e apenas refletem a manifestação de um complexo processo na perspectiva da piora da função ventricular.

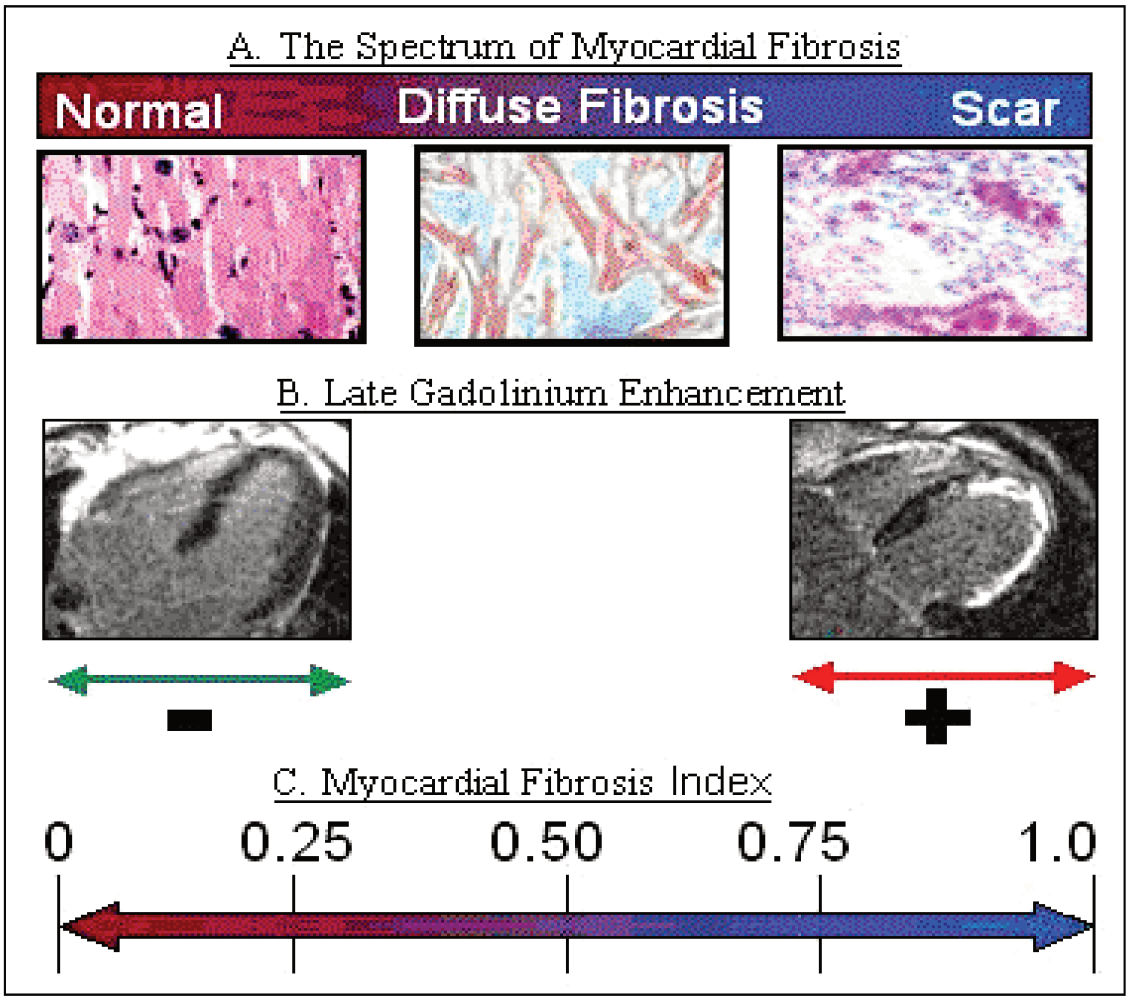

Figura 1- Espectro da fibrose miocárdica

O coeficiente de partição do gadolínio-DTPA(λGd), no miocárdio em combinação com o hematócrito sanguíneo fornece a medida continua da fração do volume extra celular, ou "índice de fibrose" **(C)**. O realce tardio **(B)** é capaz de detectar apenas áreas com fibrose densa, enquanto que o "índice da fibrose" consegue identificar um amplo espectro da fibrose miocárdica **(A)**.

1.6- Fibrose intersticial difusa e quantificação do T1 pela RMC

A primeira evidência de que a medida do coeficiente de partição do gadolínio-DTPA no miocárdio (λ_{GD}) poderia ser útil para caracterizar o remodelamento da matriz extracelular em pacientes com cardiopatia dilatada não-isquêmica foi publicado pelo Dr. Jerosch-Herold (66). Neste grupo de pacientes, o coeficiente de partição do gadolínio (λ_{GD}) e a FVEC mostraram íntima e robusta associação com o grau de dilatação ventricular assim como com o grau de disfunção sistólica do ventrículo esquerdo. Em seguida, um recente estudo do grupo liderado pelo Dr. Manning confirmou que a medição dos valores de T1 após a infusão de gadolínio era significativamente maior em pacientes com cardiopatia dilatada, quando comparado com voluntários sadios (67,68). Cumpre salientar que existem diversas vantagens na quantificação do λ_{GD} sobre a simples medida do T1 após injeção de gadolínio. Ao invés de apenas refletir o volume extracelular, a quantificação do λ_{GD} depende também de vários outros fatores como a taxa de difusão do contraste do sangue, a dosagem do contrate e o tempo em que as medidas são realizadas. Dessa forma como o λ_{GD} leva em consideração o "*arterial input"* do contraste, permitindo a quantificação de propriedades do tecido cardíaco independentemente da dosagem do contraste, do tempo, do equilíbrio entre sangue-tecido, além de dados hemodinâmicos da pressão arterial e frequência cardíaca. Em outra publicação, a simples medição do T1 após a administração de gadolínio identificou claramente pacientes com insuficiência cardíaca quando comparados a controles sem doença cardíaca (60). Neste estudo os valores anormais de T1 apresentam correlação com a expansão da matriz extracelular. Os valores de T1 também apresentaram correlação com o grau de disfunção diastólica e com a quantidade de colágeno por biópsia miocárdica. Também foi demonstrado que esta associação se mantinha mesmo quando os autores ajustavam para idade, frequência cardíaca e índice cardíaco. Conforme discutido no editorial que acompanhou a publicação (69), esse método se mostrou muito promissor, sendo "a próxima fronteira para um melhor entendimento da disfunção miocárdica". Flett et al (70) mais recentemente usaram

a abordagem semelhante a previamente descrida por Jerosch-Herold para a quantificação da FVEC, com exceção do fato de Flett ter utilizado infusão constante de contraste. O estudo publicado por Flett et al validou a quantificação da FVEC do miocárdio contra a medida do volume de colágeno obtido pela biópsia endomiocárdica, sendo que os autores reportaram um elevado grau de correlação entre essas duas medidas. No presente estudo iremos utilizar a técnica baseada na injeção de múltiplas pequenas doses de gadolínio, o que propicia medidas de T1 em diferentes concentrações de contrate circulante, proporcionando medidas de T1 muito mais precisas e reprodutíveis.

1.7- Quantificação da medida do coeficiente de partição do gadolínio no miocárdico

O coeficiente de partição para um traçador no miocárdio é definido como a razão da concentração do referido traçador no tecido e no sangue em equilíbrio. Em equilíbrio, a concentração de um contraste extracelular, como é o caso do gadolínio, no espaço intersticial deve ser igual à concentração desse contraste no sangue. Em termos de volumes específicos (volume normalizado pelo peso do tecido, expresso em ml/g) do interstício (V_{inters}) e do plasma (V_{plasma}), é possível expressar o coeficiente de partição para um traçador ou contraste extracelular como:

$$\lambda = (V_{inters} + V_{plasma})/(1\text{-Hct}) \quad (1)$$

Onde Hct é o hematócrito do sangue. Os contrastes utilizados em ressonância magnética tipicamente detectam seu efeito no sinal do H^1. Dessa forma o coeficiente de partição do gadolínio no miocárdio pode ser calculado a partir da razão entre mudanças de R1 (R1=1/T1) no tecido sobre a mudança de R1 no sangue. Diversas estratégias já foram propostas para a medida do coeficiente de partição do gadolínio no miocárdio pela RMC, sendo que a maioria desses estudos foi realizada em voluntários sem cardiopatia (58), ou em pacientes com cardiopatia isquêmica (71).

Os estudos iniciais *in-vivo* assumiram a necessidade de um longo período para obtenção de equilíbrio após administração de gadolínio entre o sangue e o tecido cardíaco (58,72,73). Apenas recentemente ficou comprovado ser possível a medida do coeficiente de partição do gadolínio no miocárdio após única administração de contraste paramagnético extracelular (0.2mmol por peso em Kg), através da aquisição combinada de imagens ponderadas em T1, medindo as mudanças na intensidade de sinal cerca de 30 minutos após a injeção do contraste (71).

1.8- Tempo de vida Intracelular da água pela RMC para detectar hipertrofia a nível celular

Os cardiomiócitos são células alongadas, próximas da forma cilíndrica (74,75). O tempo de vida intracelular das moléculas de água (TVIMA) é definido como o tempo médio para as moléculas de água cruzarem as membranas celulares (Figura 2). Sabemos que moléculas de água podem atravessar livremente a membrana celular entre o espaço intersticial (extracelular) e o espaço intracelular, sendo que o tempo médio de vida da água intracelular é o tempo de difusão para atingir a membrana celular.

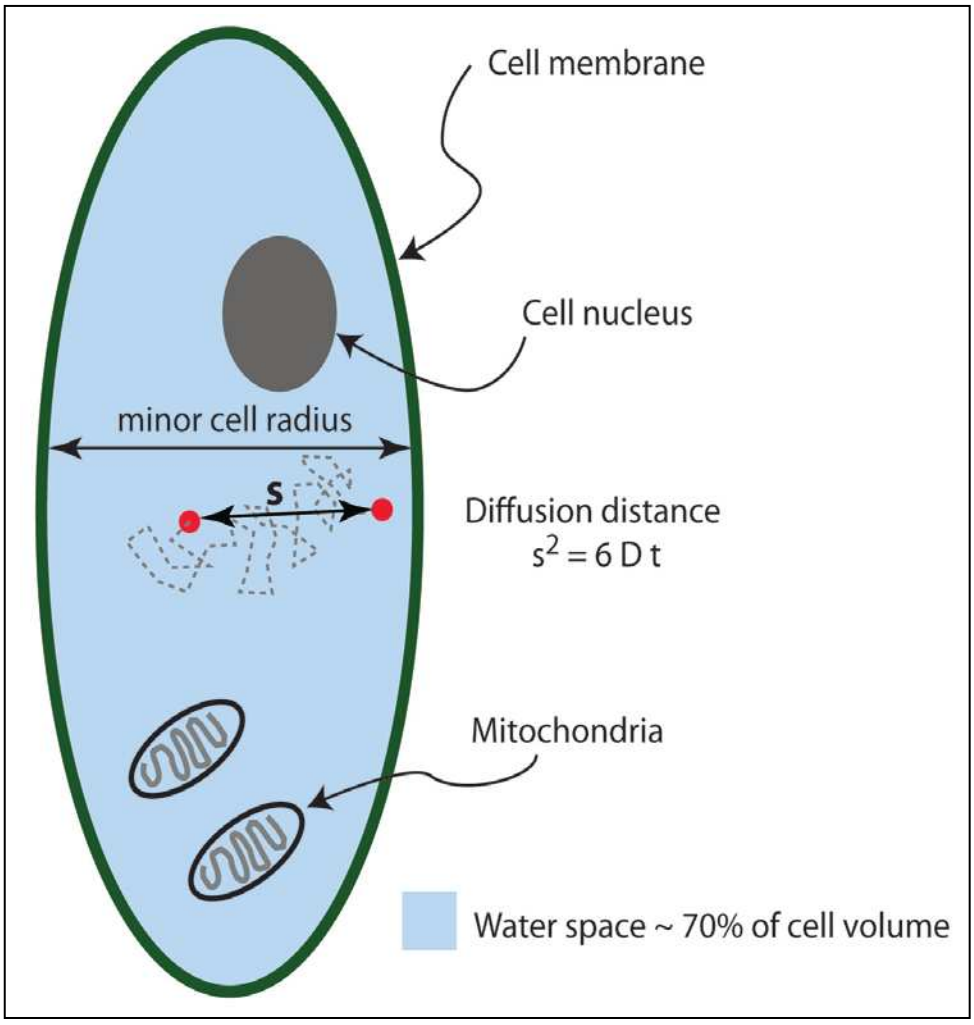

Figura 2- Tempo de vida intracelular das moléculas de água

A medida do TVIMA está diretamente relacionada ao tamanho e ao volume das células (76). Pela equação da difusão de Einstein (citado por 77), temos que **S** é a distância de difusão, **D** é o coeficiente de difusão intracelular do plasma e **t** é o tempo de difusão:

$$\mathbf{S^2 = 6\ D\ x\ t\ (2)}$$

O TVIMA teoricamente muda linearmente com relação volume para superfície. Para uma célula alongada, quase cilíndrica, o TVIMA é em uma primeira aproximação o diâmetro menor da célula.

No miocárdio, a determinação do tempo T1 após a administração de um contraste extracelular como o gadolínio-DTPA pode ser usada para investigar o TVIMA (76).

Estudos com modelos animais de hipertrofia cardíaca demonstraram que o aumento do volume dos cardiomiócitos é um marcador precoce do remodelamento cardíaco, ocorrendo em resposta a sobrecarga mecânica, na transição para insuficiência cardíaca (13,78,79). Ao nível macroscópico, o aumento da espessura e da massa do ventrículo esquerdo é o resultado da hipertrofia dos cardiomiócitos em conjunto com a expansão da matriz extracelular (80), sendo que ambos estes fatores desempenham importante papel na transição de hipertrofia compensada para insuficiência cárdica com sintomas clínicos (81).

Apesar da grande importância da hipertrofia dos cardiomiócitos e da expansão da matriz extracelular no complexo processo de remodelamento cardíaco, nenhum método de imagem até a presente data, é capaz de quantificar longitudinalmente essas duas alterações no miocárdio. Um método não invasivo com a propriedade de identificar e quantificar o hipertrofia de cardiomiócitos e a expansão da matriz extracelular pode, além de detectar eventos precoces do remodelamento cardíaco, seguir longitudinalmente o eventual efeito de intervenções terapêuticas nesses dois marcadores do remodelamento cardíaco.

Dessa forma a hipótese desse estudo é que a determinação conjunta da FVEC e do TVIMA pela RMC, através da obtenção de imagens ponderadas em T1 antes e depois da administração de gadolínio, permite a caracterização de dois importantes componentes do remodelamento do músculo cardíaco, a hipertrofia dos cardiomiócitos e a expansão da matriz extracelular.

2- OBJETIVO

O presente estudo tem como objetivo desenvolver e validar uma técnica derivada da RMC para quantificação conjunta da expansão do espaço extracelular no miocárdio, assim como da hipertrofia dos cardiomiócitos.

3- MÉTODOS E RESULTADOS

Os resultados da presente tese estão apresentados nos seguintes artigos:

1- "*Role of transcytolemmal water-exchange in magnetic resonance measurements of diffuse myocardial fibrosis in hypertensive heart disease.*", publicado no *Circulation Cardiovascular Imaging* em Janeiro de 2013 (doi: 10.1161/CIRCIMAGING.112.979815).

2- "*Quantification of Cardiomyocyte Hypertrophy by Cardiac Magnetic Resonance: Implications on Early Cardiac Remodeling*", submetido para publicação no *Circulation* e atualmente em revisão (CIRCULATIONAHA/2012/000438).

Circulation
Cardiovascular Imaging
JOURNAL OF THE AMERICAN HEART ASSOCIATION

American Heart Association
Learn and Live

Role of Transcytolemmal Water-Exchange in Magnetic Resonance Measurements of Diffuse Myocardial Fibrosis in Hypertensive Heart Disease

Otavio R. Coelho-Filho, François-Pierre Mongeon, Richard Mitchell, Heitor Moreno, Jr, Wilson Nadruz, Jr, Raymond Kwong and Michael Jerosch-Herold

Circ Cardiovasc Imaging 2013;6;134-141; originally published online November 15, 2012;
DOI: 10.1161/CIRCIMAGING.112.979815
Circulation: Cardiovascular Imaging is published by the American Heart Association. 7272 Greenville Avenue, Dallas, TX 72514
 Print ISSN: 1941-9651. Online ISSN: 1942-0080

Role of Transcytolemmal Water-Exchange in Magnetic Resonance Measurements of Diffuse Myocardial Fibrosis in Hypertensive Heart Disease

Otavio R. Coelho-Filho, MD, MPH; François-Pierre Mongeon, MD, SM; Richard Mitchell, MD, PhD; Heitor Moreno, Jr, MD, PhD; Wilson Nadruz, Jr, MD, PhD; Raymond Kwong, MD, MPH; Michael Jerosch-Herold, PhD

Background—The myocardial extracellular volume fraction (MECVF) has been used to detect diffuse fibrosis. Estimation of MECVF relies on quantification of the T1 relaxation time after contrast enhancement, which can be sensitive to equilibrium transcytolemmal water-exchange. We hypothesized that MECVF, quantified with a parsimonious 2-space water-exchange model, correlates positively with the connective tissue volume fraction in a rodent model of hypertensive heart disease, whereas the widely used analysis based on assuming fast transcytolemmal water-exchange could result in a significant underestimate of MECVF.

Methods and Results—Nω–nitro-L-arginine-methyl-ester (L-NAME) or placebo was administered to 22 and 15 wild-type mice, respectively. MECVF was measured at baseline and 7-week follow-up by pre- and postcontrast T1 cardiac magnetic resonance imaging at 4.7 T, using a 2-space water-exchange model. Connective tissue volume fraction was quantified, using Masson trichrome stain. L-NAME induced hypertrophy (weight-indexed left-ventricular mass 2.2±0.3 versus 4.1±0.4 μg/g, $P<0.001$), and increased connective tissue volume fraction (8.6%±1.5 versus 2.58%±0.6, $P<0.001$), were compared with controls. MECVF was higher in L-NAME-treated animals (0.43±0.09 versus 0.26±0.03, $P<0.001$), and correlated with connective tissue volume fraction and weight-indexed left-ventricular mass ($r=0.842$ and $r=0.737$, respectively, both $P<0.0001$). Neglecting transcytolemmal water-exchange caused a significant underestimate of MECVF changes. Ten patients with history of hypertension had significantly higher MECVF (0.446±0.063) compared with healthy controls (0.307±0.030, $P<0.001$).

Conclusions—Cardiac magnetic resonance allowed detection of myocardial extracellular matrix expansion in a mouse model and in patients with a history of hypertension. Accounting for the effects of transcytolemmal water-exchange can result in a substantial difference of MECVF, compared with assuming fast transcytolemmal water-exchange. (***Circ Cardiovasc Imaging*. 2013;6:134-141.**)

Key Words: cardiac magnetic resonance ■ extracellular volume fraction ■ gadolinium-DTPA ■ mice ■ myocardial fibrosis ■ Nω–nitro-L-arginine-methyl-ester ■ transcytolemmal ■ water-exchange

Late gadolinium enhancement imaging (LGE) has become the method of choice to detect myocardial necrosis and scar with cardiac magnetic resonance (CMR), yet LGE may provide only a partial measure of fibrosis extent and burden, as it relies on a difference in signal intensity that may not exist in the case of diffuse and generalized fibrosis.

Clinical Perspective on p 141

Conditions such as nonischemic dilated, diabetic, and hypertrophic cardiomyopathies, along with hypertensive and valvular heart disease, have shown ample histopathologic evidence of diffuse fibrosis.[1–3] Diffuse myocardial fibrosis is an important, yet poorly characterized substrate for sudden cardiac death.[4] It is associated with the development of heart failure in hypertensive patients[5] and may regress under treatment.[6]

A shorter myocardial T1 after administration of an extracellular gadolinium-based contrast agent indicates extracellular matrix expansion and is associated with accumulation of connective tissue in the myocardium.[7] Flett et al[8] demonstrated that the extracellular volume correlates with the collagen volume fraction in patients with aortic stenosis and hypertrophic cardiomyopathy.

CMR estimation of extracellular matrix expansion relies on the indirect detection of contrast in tissue and on its effect on T1 relaxation times. T1 of tissue represents the time constant for the inversion recovery of water within the entire tissue

Received August 12, 2012; accepted October 17, 2012.

From the Cardiovascular Division (O.R.C-F., F-P.M., R.K.), Department of Radiology (M.J-H.), Department of Pathology (R.M.), Brigham and Women's Hospital, Boston, MA; Department of Internal Medicine, State University of Campinas (UNICAMP), Sao Paulo, Brazil (O.R.C-F., H.M., W.N.); and Department of Medicine, Montreal Heart Institute, Université de Montréal, Montreal, Canada (F-P.M.).

Guest Editor for this article was David A. Bluemke, MD, PhD.

Correspondence to Michael Jerosch-Herold, PhD, Department of Radiology, Brigham and Women's Hospital, 75 Francis St, Radiology BWH Box 22, Boston, MA-02115. E-mail mjerosch-herold@partners.org

Circ Cardiovasc Imaging **is available at http://circimaging.ahajournals.org** **DOI: 10.1161/CIRCIMAGING.112.979815**

space, not only the space permeated by contrast. In structures where contrast agents are confined to subspaces, while water diffuses between all the subspaces, T1 depends on the rate at which water exchanges between the spaces with and without contrast, eg, across the cytolemmal barrier between extra- and intracellular spaces.[9–11]

Previous CMR studies of the myocardial extracellular volume fraction (MECVF) in aortic stenosis and hypertrophic cardiomyopathy,[8] idiopathic dilated cardiomyopathy,[12] congenital heart disease,[13] and healthy volunteers[14] were all based on assuming fast transcytolemal water-exchange, which predicts a linear relationship between the relaxation rates, R1 (=1/T1), in myocardium and blood, before and after contrast enhancement. When the myocardial relaxation times are sufficiently reduced by contrast administration,[11] the relationship between R1 in myocardial tissue and R1 in blood will change from linear to sublinear.[11] Continuing to assume, that after contrast administration the transcytolemmal water-exchange remains fast, can result in a significant underestimate of MECVF. By measuring myocardial R1 after consecutive contrast injections, one can detect the deviation from a linear relationship for R1 in myocardium and blood, and determine the underestimate of MECVF, resulting from the assumption of fast transcytolemmal water-exchange.

We hypothesized that MECVF, quantified with a parsimonious 2-space water-exchange (2SX) model,[11] correlates positively with the connective tissue volume fraction (CTVF) in a rodent model of hypertensive heart disease, induced by chronic inhibition of NO biosynthesis with Nω–nitro-L-arginine-methyl-ester (L-NAME), whereas the widely used analysis based on assuming fast exchange (FX) across the cytolemmal barrier could result in a loss of sensitivity to MECVF expansion. The same CMR approach was also tested in hypertensive patients without overt signs of myocardial hypertrophy, and volunteers, to determine whether MECVF could be used as an early marker of adverse extracellular matrix remodeling.

Methods

Animal Experimental Groups

Thirty-seven male wild-type mice (mean body-weight 37.6±2.5 g, range 30–40 g, Taconic, Germantown, NY) were randomly assigned to 1 of 2 experimental groups: (1) Placebo-treated (control group; n=15), receiving tap water alone for 7 weeks, and (2) L-NAME-treated (L-NAME group; n=22) with L-NAME in the drinking water (3 mg/mL; Sigma) for 7 weeks. Animals were kept under standard conditions and had normal food and water ad libitum. Noninvasive tail blood pressures were obtained at baseline and weekly after treatment started, using a volume–pressure recording tail-cuff technique[15] (CODA-1, Kent Scientific, Torrington, CT). CMR was performed at baseline and after 7 weeks of treatment. Retro-orbital blood sampling was performed immediately after each CMR study for hematocrit determination (i-STAT, Abbott, IL). Animals were killed after the second CMR study, and the hearts were excised for histological analysis. The study protocol and animal care conformed with the Guide for the Care and Use of Laboratory Animals from the National Institutes of Health (NIH Publication No. 85-23, Revised 1996). The study protocol was approved by the Standing Committee on Animal Care and Use at Harvard University.

Histological Analysis

Heart tissues were fixed with buffered 10% formalin solution (Fisher Scientific, Pittsburgh, PA). Short-axis cuts (≈1 mm thickness) of formalin fixed tissue were processed, embedded in paraffin, and stained with standard hematoxylin, eosin, and Masson trichrome. All sections were scanned with ScanScope scanners (Aperio Technologies, Inc; Vista, CA). Whole-slide images were downsampled to a resolution of 1.0 μm/pixel. Pixels stained in blue with Masson trichrome were identified for quantification of CTVF, using a semiautomatic pixel color intensity algorithm.

Patient Population

CMR was performed on 8 consecutive patients referred clinically with a diagnosis of hypertension (HTN) and evidence of hypertensive heart disease defined as increased wall thickness or left atrial enlargement, confirmed by CMR. Patients were also required to have normal left-ventricular (LV) systolic function ≥50%, no LGE and no significant valvular heart disease. All CMR studies were clinically requested and indicated, and no patient received gadolinium for the sole purpose of the study. Our institutional review board approved this study for review of patient's records. In addition, CMR data from 12 healthy volunteers using identical imaging parameters were obtained as control group. Healthy volunteers had signed informed consent for the institutional review board-approved research protocol before undergoing CMR.

Clinical, Electrocardiographic Data

Clinical history was collected at the time of CMR. Electrocardiograms closest in time to CMR were reviewed. LV filling pressure was assessed by tissue Doppler imaging using the ratio (≥15) of the peak velocity of the mitral E wave to the peak velocity of the E' wave of the basal lateral, and septal wall (mitral annulus). A decreasing peak velocity of the E' wave at the mitral annulus by tissue Doppler imaging was also used as an indicator of the severity of diastolic dysfunction.[4]

CMR Imaging Protocols

Mice

Animals were imaged supine under isofluorane anesthesia (induction 4%–5%; maintenance 1%–2.5% in oxygen from a precision vaporizer) in a 4.7-T MRI system (BioSpec 47/40, Bruker BioSpin, Billerica, MA). Mice were placed in a special cradle, ECG electrodes fixed to front and back paws, using electrode gel to optimize electric contact. For ventricular size and function, cine gradient-echo images were acquired (repetition time [TR]=5.9 ms; echo time [TE]=2.2 ms; temporal resolution =20–30 ms; in-plane spatial resolution 100–120 × 180–210 μm; 1 mm thick) in multiple parallel short-axis. Gadolinium diethylenetriamine pent-acetic acid (DTPA, Magnevist, Berlex, Wayne, NJ) was injected subcutaneously in multiple steps up to a cumulative dose of 0.5 mmol/kg. T1 was measured precontrast, and after each of 4 to 5 contrast injections with a modified Look-Locker technique, no earlier than 6 minutes after each contrast administration, using the following parameters: TR =2.5 ms; TE =1.8 ms; flip angle =15°, in-plane resolution 190 μm, slice thickness 1 mm; repetition time per segment: 22 ms; number of averages: 6 (precontrast), or 4 (postcontrast). An adiabatic hyperbolic secant pulse was applied for nonslice-selective magnetization inversion before each Look-Locker magnetization-recovery read-out. The accuracy of the T1 measurements was tested in gadolinium-doped phantoms, against the standard inversion recovery spin-echo technique.

Patients

Patients were studied supine position in a 3.0-T MRI system (Tim Trio, Siemens Medical Systems, Malvern, PA). For LV size and function, a cine steady-state free-precession sequence was used (TR =3.4 ms; TE =1.2 ms; temporal resolution =40–50 ms; in-plane spatial resolution =1.5–1.8 × 1.8–2.1 mm; slice=8 mm; no gaps) in multiple

parallel short-axis. An inversion recovery-prepared fast gradient-echo sequence, triggered every other heartbeat, was used to assess for LGE in all short-axis locations, matching those for cine imaging 10 minutes after of a cumulative dose of 0.15 mmol/kg of gadolinium DTPA (Magnevist, Berlex, Wayne, NJ). T1 measurements were performed with a modified Look-Locker sequence[15] with a nonslice-selective adiabatic inversion pulse, followed by segmented gradient-echo acquisition for 17 cardiac phases/times after inversion (TI's), spread over 1 to 2 cardiac cycles (temporal resolution 105 ms precontrast, and 54 ms postcontrast, slice thickness 8 mm, TR >3 R-wave to R-wave (RR) intervals precontrast, and 2 RR intervals postcontrast). The Look-Locker sequence was repeated in the same mid LV short-axis slice, once before, and 3 additional times after the injection of gadolinium, starting at 4 minutes after injection and spanning a 30-minute period. Acquisition time with breath-holding was <20 s/slice.

Quantification of Global and Segmental MECVF

For Look-Locker images, the endo- and epicardial borders of the LV were manually drawn (QMass MR 7.1 software, Medis, The Netherlands). The signal intensity versus time curves for each segment and the blood pool were used to determine segmental T1 by nonlinear least-squares fitting to an analytic expression for the magnitude signal measured during the inversion recovery, and correction for the radiofrequency pulse effects on the inversion recovery. The reciprocal of T1 (R1) was used to plot the myocardial R1 against the R1 in the blood pool and fit with a 2SX model of equilibrium transcytolemmal water-exchange, originally developed by Landis et al.[11,16] (This model was originally referred to as a 2-site model, where the sites can be identified in the present application as the extra- and intracellular spaces, respectively.) In the limit of FX, the analytic model used for the data fits can be well approximated by a linear relationship.[8,12] (FX is defined as the regimen where the rate of transcytolemmal water-exchange is much higher than the difference of R1's in the intra- and extracellular spaces.) In the FX limit, the slope of the linear relationship between myocardial R1 and blood pool R1 defines the partition coefficient for gadolinium, λ_{Gd}. MECVF was obtained by multiplying each of the segmental λ_{Gd} by (1-hematocrit in percent/100). In the 2SX,[11,16] the MECVF, and the intracellular lifetime are adjustable parameters, optimized with a nonlinear orthogonal distance regression algorithm, and blood hematocrit was fixed at the measured value. The results obtained with the 2SX model were compared with the MECVF estimates from the more common FX model.

Cine CMR Assessment

Manually traced epicardial and endocardial borders of matching short-axis cine locations at end systole and end diastole were used to determine the LV ejection fraction, LV end-diastolic volume index, LV end-systolic volume index, and LV myocardial mass (end diastole only). Left atrial area were traced in 4-chamber and 2-chamber views in human subjects to calculate the biplane left atrial volume, which was indexed to body surface area.

Statistical Analyses

Continuous data were expressed as means±SD. Continuous variables were compared between different groups using *t* tests. Paired *t* test was used to compare continuous measurements at baseline and follow-up within a group. Bland-Altman analysis was used to compare 2 methods (eg, for estimating MECVF, or measuring R1), and obtain the 5% and 95% limits of agreement. Multivariate linear regression analysis was performed to assess the association of the difference of MECVF values from 2SX and FX models, with the maximum R1 in blood and the LV mass index. A log-likelihood ratio test was used to compare the fits with the 2SX and FX models. The likelihood ratio was tested for statistical significance by assuming that it is asymptotically χ^2 distributed with degrees of freedom equal to the difference in adjustable parameters between models.

Dichotomous data were compared using a Fisher exact test when possible, and with a χ^2 test otherwise. Spearman rank correlation was used to assess statistical dependence between variables. All analyses were performed with SAS 9.2 (SAS Institute, Inc, Cary, NC) and R (version 2.13.1, R Foundation for Statistical Computing, Vienna, Austria, 2011, URL: http://www.R-project.org).

The authors had full access to and take full responsibility for the integrity of the data. All authors have read and agreed to the article as written.

Results

Animal Hemodynamic Data

Table 1 summarizes the hemodynamic and left-ventricular parameters for the L-NAME and control groups. At baseline, control, and L-NAME groups did not show any significant differences in body-weight, blood pressure, heart rate, and CMR-derived data (Table 1).[17–19] The chronic administration of L-NAME was associated with a significant increase in the mean blood pressure.[17–19]

Table 1. Baseline and Follow-Up Characteristics and CMR Data

	Baseline			7-week		
Characteristics	Control (n=15)	L-NAME (n=22)	*P**	Control (n=15)	L-NAME (n=22)	*P**
Body-weight, g	37.6±2.5	36.9±2.3	0.359	44.3±4.3‖	39.9±2.1‖	0.001
HR, bpm	510.8±112.4	485.0±73.7	0.442	472.1±59.9	446.6±47.5	0.212
Mean-BP, mm Hg	92.9±7.2	89.0±6.4	0.216	91.4±6.2	127.2±6.1‖	<0.001
LVEF, %	57.8±3.7	58.7±2.9	0.405	60.3±3.2	51.3±8.2§	<0.001
LVEDV, μL	128.2±30.1	142.8±34.6	0.195	110.6±26.2	117.9±34.3†	0.531
LVESV, μL	54.05±13.1	59.1±15.5	0.310	44.1±12.0†	57.2±19.1	0.029
LV mass, μg	94.5±16.3	92.6±12.4	0.699	98.5±14.4	162.9±19.4‖	<0.001
LV mass index to body-weight, μg/g	2.5±0.4	2.5±0.3	0.989	2.2±0.3	4.1±0.4‖	<0.001
MECVF	0.269±0.034	0.2645±0.046	0.791	0.267±0.033	0.4139±0.086‖	<0.001

BP indicates blood pressure; CMR, cardiac magnetic resonance; HR, heart rate; LV, left ventricular; LVEDV, left-ventricular end-diastolic volume; LVEF, left-ventricular ejection fraction; LVESV, left-ventricular end-systolic volume; and MECVF, the myocardial extracellular volume fraction.

*Control vs L-NAME mice, unpaired *t* test.

†P<0.05; ‡P<0.01; §P<0.005; ‖P<0.001, baseline vs 7-week mice paired by group (control and L-NAME), paired *t* test.

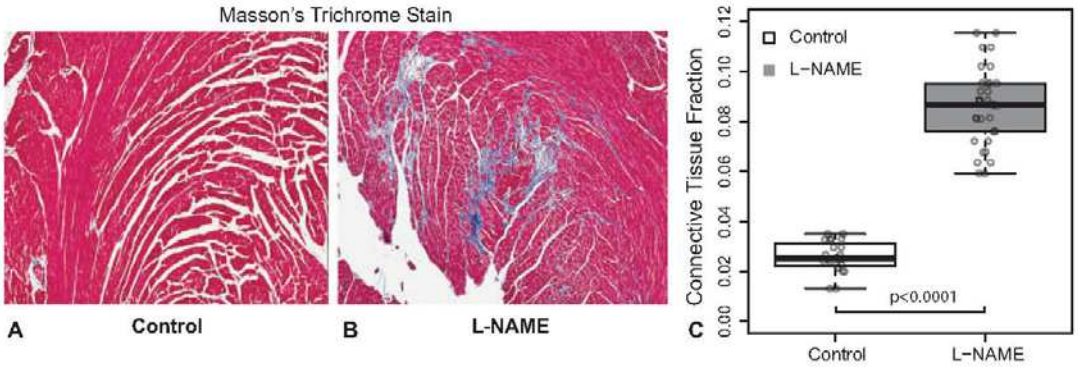

Figure 1. Representative examples of myocardial tissue stained with Masson trichrome in a midlevel myocardial slice from the control group (**A**) and the L-NAME group (**B**) shows a visually clear difference of blue-colored, connective tissue. Connective tissue fraction, shown in (**C**), and defined as the number of pixels with a bluish hue, divided by the total number of myocardial pixels in the slice, was significantly different between controls and L-NAME treated mice.

Histological and CMR Markers of Fibrosis

At follow-up, the CTVF was significantly higher in the L-NAME group compared with placebo-treated mice (8.6%±1.5 versus 2.58%±0.6, $P<0.001$), as shown in Figure 1. This was mirrored with CMR by an increased MECVF in the L-NAME-treated animals, compared with controls (0.43±0.09 versus 0.26±0.03, $P<0.001$). The myocardial R1 showed a noticeable sublinear dependence on R1 in blood, as exemplified for an L-NAME treated mouse in Figure 2A. The 2SX model resulted in better fits to the data ($P<0.05$ for likelihood ratio test), compared with the linear FX model, in 77% of the L-NAME cases, and in 35% of the cases with placebo or before L-NAME treatment. Figure 2B shows that MECVF from the 2SX model correlated with the connective tissue fraction ($r=0.737$ $P<0.0001$), whereas MECVF from FX model did not correlate with CTVF ($P=0.44$). Bland-Altman analysis showed that the FX model fit can cause a significant underestimate MECVF expansion (mean difference: –0.068; 5%, and 95% limits of agreement: –0.051 to –0.085). The percent bias (difference/mean in %) to underestimate MECVF with the FX model became larger with extracellular matrix expansion, LV hypertrophy, and increased with the range of R1 in blood, covered by the measurements ($P<0.001$). This was tested statistically with a multivariable linear regression model for the % MECVF difference, with the mean MECVF, the maximum R1 in blood ($P<0.002$), and LV mass index ($P<0.002$) included as predictors. A separate analysis shows that estimates of MECVF obtained with FX model over a low, restricted R1 range (R1 in blood $<2\ s^{-1}$) agree with the 2SX model within –0.003 (5% and 95% limits of agreement: 0.076–0.07). All further results for MECVF refer to the MECVF obtained with the 2SX model over the full range covered of R1 measurements. The mean MECVF at baseline did not differ between L-NAME and control mice (0.2645±0.046 versus 0.269±0.034, $P=0.719$, Figure 3A).

Seven studies with 2 consecutive T1 measurements without intermediate contrast injection were used to estimate the half life ($t_{1/2}$) for Gd clearance after subcutaneous injections. The range of times between the 2 T1 measurements averaged 21 minutes (range: 7–33 minutes.). The $t_{1/2}$ was 70±16 minutes (mean±SD)

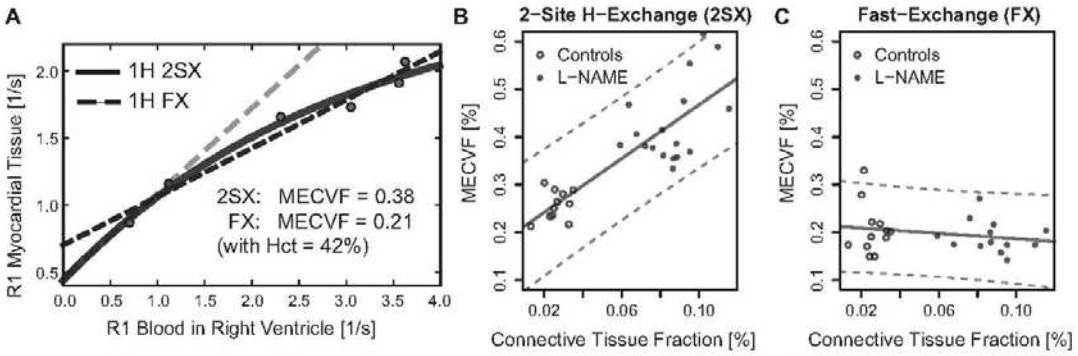

Figure 2. A, The relation between myocardial R1 and blood pool R1 was fit with a 2-space 1H exchange model (2SX), to account for transcytolemmal water-exchange (solid black line). Assuming fast water-exchange (FX) predicts a linear relationship between myocardial R1 and blood R1. For lower R1 values (gray dashed line) this gives reasonable agreement, but results in an 80% underestimate of MECVF (0.38 vs 0.21) if the FX model is used over the entire R1 range (black dashed line). **B**, MECVF correlated significantly with the connective tissue fraction obtained from myocardial slices stained with Masson trichrome stain. **C**, No significant correlation could be observed when the R1 relationship was analyzed with the fast 1H exchange assumption. MECVF indicates myocardial extracellular volume fraction.

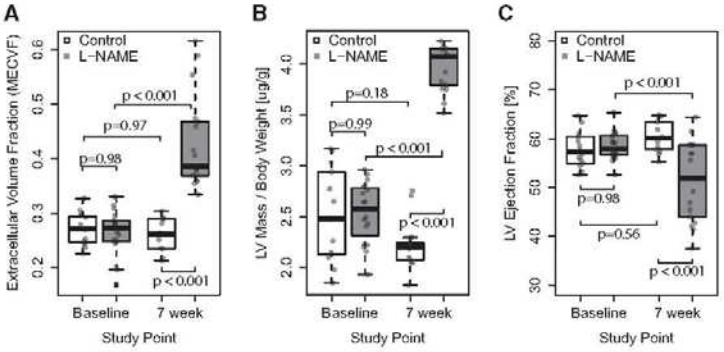

Figure 3. Chronic L-NAME treatment caused myocardial extracellular volume expansion (**A**), increased left-ventricular (LV) mass indexed to body-weight significantly (**B**), and significantly reduced LV ejection fraction (**C**). Data were analyzed by *t* test and paired *t* test as appropriate.

after subcutaneous injections of contrast, sufficiently long to allow for contrast equilibrium between blood and tissue.

R1 measurements at 4.7 T with the Look-Locker technique were compared against a standard IR-prepared spin-echo technique in 10 gadolinium-doped phantoms with R1 ranging from 0.35 to 8.4 s^{-1}. The mean difference (R1 from IR cine – R1 from IR-SE) was –0.01±0.09 s^{-1}, with the 5% and 95% limits of agreement obtained by Bland-Altman analysis at –0.19 s^{-1} and 0.16 s^{-1}. For 3T (Siemens Trio), the mean difference of R1 in 10 phantoms, using the Look-Locker and IR-spin-echo techniques was –0.093 s^{-1} (Bland-Altman 5% and 95% limits of agreement: –0.44 to 0.27), with the mean R1 covering a range from 0.795 to 6.7 s^{-1}.

Morphological and Functional Changes Associated with Chronic L-NAME treatment

Treatment with L-NAME for 7 weeks was associated with a significant increase in cardiac mass (92.6±12.4 versus 162.9±19.4 μg, $P<0.001$) and reduction in LV ejection fraction (58.7±2.9% versus 51.4±8.2%, $P=0.003$, Figure 3B and 3C). At follow-up, MECVF correlated significantly with mean arterial pressure, LV ejection fraction, and LV mass indexed with body-weight (Figure 4). Similarly, CTVF correlated with mean arterial pressure ($\rho=0.76$; $P<0.001$), LV ejection fraction ($\rho=-0.52$; $P<0.004$), and LV mass index ($\rho=-0.67$; $P<0.004$).

Pilot Data From a Cohort of Hypertensive Patients

Patients with treated HTN tended ($P=0.136$) to be older than healthy volunteers (Table 2). There was no substantial difference in systolic and diastolic blood pressure between volunteers and HTN patients (Table 2). Among HTN patients, 6 (60%) took a calcium channel blocker, 5 (50%) took a β-blocker, 5 (50%) took an angiotensin-converting enzyme inhibitor or an angiotensin receptor blocker, and 4 (40%) took a diuretic. LV hypertrophy on ECG was present in 3 (30%) patients, suggesting that increased MECVF can occur without common signs of hypertensive heart disease. Echocardiograms were available in 8 HTN patients. Among them, the mean E/E' ratio was 11.6±2.1 at the basal lateral wall and 16.6±4.8 at the basal septal wall, indicating high LV filling pressure. By CMR, LV volumes, mass, and function were not substantially different between HTN patients and volunteers (Table 2). Biplane left atrial volume index was substantially higher in HTN patients than in volunteers (Table 2). Half of the patients had thickened LV walls (≥12 mm in men and ≥10 mm in women).[20] The dependence of the myocardial R1 on R1 of blood showed a similar sublinear dependence (Figure 5) using a standard clinical contrast dosage (≤0.2 mmol/kg). The deviation from the linear FX model had similar effects, as observed in the experimental studies. The MECVF for all patients and volunteers correlated significantly with left atrial volume ($\rho=0.58$, $P=0.008$).

Discussion

CMR showed significant MECVF expansion as a result of arterial HTN from inhibition of NO synthesis by chronic administration of L-NAME. The expansion of the extracellular matrix, and myocardial hypertrophy, can exacerbate the

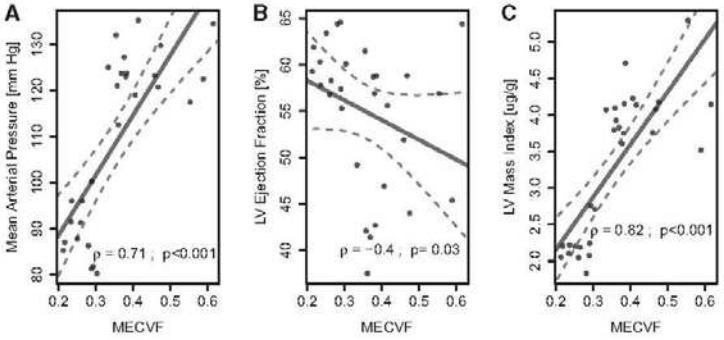

Figure 4. Correlations (Spearman's ρ) between the myocardial extracellular volume fraction (MECVF) and (**A**) mean blood pressure (7 weeks), (**B**) left-ventricular (LV) ejection fraction, and (**C**) LV mass indexed by body-weight.

Table 2. Clinical and CMR Characteristics of Human Subjects Cohort

	Hypertension	Normal	*P*
Number	8	12	
Age	66.2±16.3	56.3±5.2	0.136
Weight, kg	89.6±30.4	76.4±17.9	0.294
Body surface area, m^2	2.047±0.198	1.874±0.358	0.241
Female	2 (25%)	7 (58%)	0.310
Systolic BP, mm Hg	133±10.7	125.1±10.5	0.118
Diastolic BP, mm Hg	70±13.4	78.1±7.1	0.162
NYHA class ≥ II	5 (62.5%)	0	<0.001
LVEDV index, mL/m^2	72.5±17.6	67.6±14.0	0.521
LVESV index, mL/m^2	67.0±19.4	25.7±7.5	0.487
LVEF, %	62.1±8.9	62.3±5.2	0.746
LV mass index, g/m^2	49.9±12.1	45.1±6.8	0.331
Biplane LA volume, mL/m^2	32.61±20.12	12.98±5.35	0.028
Myocardial extracellular volume fraction (2SX model)	0.446±0.063	0.307±0.030	0.0002
Myocardial extracellular volume fraction (FX model)	0.332±0.045*	0.263±0.027*	0.004

BP indicates blood pressure; LV, left ventricular; LVEDV, left-ventricular end-diastolic volume; LVEF, left-ventricular ejection fraction; LVESV, left-ventricular end-systolic volume; and NYHA, New York Heart Association.

*P<0.01 for paired t test of 2-site water-exchange model (2SX) and against standard fast exchange model (FX).

bias to underestimate of MECVF if the effect of transcytolemmal water-exchange on myocardial T1 is neglected. With the use of a parsimonious 2SX model, the estimate of MECVF resulted in a good correlation with histological measurements of the connective tissue fraction, using Masson trichrome staining. Using this model, we found significant extracellular matrix expansion in patients with treated hypertension, undetected by LV mass index, or LGE imaging. Increased MECVF correlates strongly with the left atrial volume index in patients, which supports the pathophysiologically plausible role of diffuse fibrosis in ventricular stiffening.

The CMR-derived MECVF was previously validated against collagen volume fraction determined by picrosirius red staining.[8,21] Picrosirius red is a relatively sensitive way to identify collagens in dense fibrosis, particularly type I collagen; the characteristic red stain under polarized light provides a strong signal, and fibril orientation is easily demonstrated. However, with lesser amounts of extracellular fibrosis, or at earlier stages of deposition when glycosaminoglycans, proteoglycans, fibronectin, and type III collagen predominate, picrosirius is an insensitive method to assess matrix content. Thus, we have used Masson trichrome to highlight and quantify all elements of the extracellular matrix, including the noncollagenous components. Myocardium lends itself well to the Masson stain because the usual matrix content is low. There is a distinct colorimetric difference between myocytes and fibrosis.

Transcytolemmal water-exchange plays an important role in determining myocardial T1 when an extracellular contrast agent creates a difference of R1 rates between intra- and extracellular spaces on the order of the transcytolemmal water-exchange rate. A parsimonious 2SX model was previously worked out in detail and validated.[11,16] The potential benefits of using this model for estimating MECVF was not considered before. The 2SX model predicts a sublinear dependence of R1 in tissue on R1 in blood (plasma), and the degree of curvature is determined by the intracellular lifetime of water, and the R1 range in blood (plasma) covered by the T1 measurements. The intracellular lifetime reflects a tissue property that is stable with homeostasis, and there is no evidence that it changes with gadolinium contrast administration.

The less than linear increase of the myocardial R1 as a function of R1 in blood results in a systematic underestimate of MECVF, if the data are analyzed with a linear FX model (Figures 2 and 5). The bias introduced by assuming FX was observed to increase significantly with MECVF and intracellular lifetime, and also depended on the range of R1 values in blood. The better fit with the 2SX model was most apparent in the L-NAME-treated mice, which probably

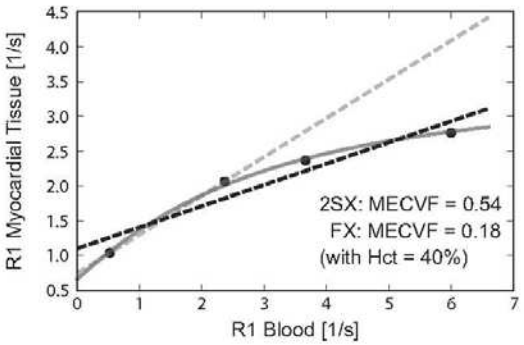

Figure 5. In an 82-year-old male with a history of hypertension, and no evidence of ischemic heart disease, myocardial R1 vs blood R1 was fit with a 2-space 1H exchange model (2SX), shown as solid line. Similarly to Figure 2, the myocardial R1 initially increases linearly (shown as gray dashed line, extrapolated to larger R1 values), and then develops a convex shape as the rate of transcytolemmal moves away from the fast exchange condition. If all R1 data points are included for a fit with a linear model, one obtains a 67% lower value for myocardial extracellular volume fraction (MECVF) (0.18), compared with the analysis with the 2SX model (0.54).

reflects the substantial development of hypertrophy and interstitial fibrosis, compared with controls. The values for the transcytolemmal (first-order) water-exchange rate constants (median =19 Hz, interquartile range =9–24 Hz) obtained in this study with the 2-space model of Landis[11,16] are within the range reported for myocardium in previous studies.[22–24]

The values of MECVF for mice in this study fall within the normal range measured in healthy human volunteers. MECVF and cardiomyocyte size or volume (≈24 ×·10^3 μm^3 in young adult male humans,[25] and 25 ×·10^3 μm^3 in mice)[26] are expected to be relatively similar across species, although they are affected by age and sex.[25]

The hypertensive patients were selected to include only those with LV mass within the sex-specific normal range, but the MECVF was significantly higher than in controls. A higher than normal LV mass is currently an accepted sign of hypertensive heart disease, if other causes of hypertrophy can be excluded. The CMR measurements may suggest that expansion of the extracellular space could precede a significant increase of LV mass. The latter may in fact represent the combined effect of extracellular matrix expansion and cell hypertrophy. Drug therapies that can achieve regression of LV hypertrophy, such as angiotensin-converting enzyme inhibitors, may benefit from an earliest possible application. MECVF could become an early marker of adverse myocardial remodeling.

The methodology for the measurements and postprocessing were essentially similar for the studies in mice and humans. The differences relate mostly to requirements for higher spatial and temporal resolution in mice compared with humans. For the mouse studies, the acquisition of the k-space segments was kept to <20 ms to avoid motion artifacts. Subcutaneous contrast injections for the mice resulted in a sufficiently slow blood clearance to assure equilibrium conditions. Importantly, accounting for the effects of water-exchange had a significant effect for both the mouse and human studies, even though the latter were based on a clinically acceptable gadolinium contrast dosage of 0.15 mmol/kg.

Limitations

The use of MECVF as a marker of fibrosis assumes that a pathological expansion of the extracellular matrix is coupled with a build-up of connective tissue, which was quantified in this study by Masson trichrome stain. Although a correlation between extracellular space expansion and CTVF is not unexpected, the characteristics of such a relationship can also be affected by the density of connective tissue in the extracellular space. The effect of connective tissue density on MECVF measurements remains unclear at this point.[8]

A further limitation is the absence of any measurements of diastolic function indices in the mouse model. For the mice, we note that there is a significant association between systolic function and MECVF.

Our observation of a significant underestimation of MECVF, when based on the FX assumption of water exchange applies mostly to protocols where R1 in the blood after contrast administration is relatively high. For R1 in blood <≈2.0 s^{-1} the percent underestimation of MECVF with the FX assumption is, in our experience, generally <≈5%, but may vary by presence and degree of hypertrophy. In this study, the maximum R1 in blood in each mouse averaged 5 s^{-1}. The findings from the comparison of MECVF obtained with the 2SX and the FX models are dependent on the contrast dosages, and the cumulative effect of contrast injections on R1 in the blood.

Conclusion

MECVF, quantified by CMR T1 measurements, detects myocardial extracellular matrix expansion, a marker of interstitial fibrosis, in a mouse model of hypertensive heart disease. The analysis of the myocardial T1 data with the assumption that transcytolemmal exchange remains in the fast exchange limit after contrast administration can result in a significant underestimation of MECVF. Underestimates of MECVF attributed to the FX assumption depend on the degree of LV hypertrophy and the maximum T1 in the blood pool. A generalization of the model for determination of MECVF may allow a more sensitive detection of diffuse fibrosis in patients with hypertension, compared with healthy controls.

Sources of Funding

The research reported in this publication was supported by the National Heart, Lung, and Blood Institute of the National Institutes of Health under Award Number R01HL090634. Dr Coelho-Filho was supported by a research grant from American Heart Association (AHA 11POST5550053), and Dr Kwong by a research grant from the National Institutes of Health (NIH RO1 HL 091157).

Disclosures

Dr Jerosch-Herold is listed as coinventor on a pending patent application related to detection of diffuse fibrosis by MRI.

References

1. Connelly KA, Kelly DJ, Zhang Y, Prior DL, Martin J, Cox AJ, Thai K, Feneley MP, Tsoporis J, White KE, Krum H, Gilbert RE. Functional, structural and molecular aspects of diastolic heart failure in the diabetic (mRen-2)27 rat. *Cardiovasc Res*. 2007;76:280–291.
2. Olivetti G, Melissari M, Balbi T, Quaini F, Cigola E, Sonnenblick EH, Anversa P. Myocyte cellular hypertrophy is responsible for ventricular remodelling in the hypertrophied heart of middle aged individuals in the absence of cardiac failure. *Cardiovasc Res*. 1994;28:1199–1208.
3. Rossi MA. Pathologic fibrosis and connective tissue matrix in left ventricular hypertrophy due to chronic arterial hypertension in humans. *J Hypertens*. 1998;16:1031–1041.
4. John BT, Tamarappoo BK, Titus JL, Edwards WD, Shen WK, Chugh SS. Global remodeling of the ventricular interstitium in idiopathic myocardial fibrosis and sudden cardiac death. *Heart Rhythm*. 2004;1:141–149.
5. Querejeta R, López B, González A, Sánchez E, Larman M, Martínez Ubago JL, Díez J. Increased collagen type I synthesis in patients with heart failure of hypertensive origin: relation to myocardial fibrosis. *Circulation*. 2004;110:1263–1268.
6. Díez J, Querejeta R, López B, González A, Larman M, Martínez Ubago JL. Losartan-dependent regression of myocardial fibrosis is associated with reduction of left ventricular chamber stiffness in hypertensive patients. *Circulation*. 2002;105:2512–2517.
7. Iles L, Pfluger H, Phrommintikul A, Cherayath J, Aksit P, Gupta SN, Kaye DM, Taylor AJ. Evaluation of diffuse myocardial fibrosis in heart failure with cardiac magnetic resonance contrast-enhanced T1 mapping. *J Am Coll Cardiol*. 2008;52:1574–1580.
8. Flett AS, Hayward MP, Ashworth MT, Hansen MS, Taylor AM, Elliott PM, McGregor C, Moon JC. Equilibrium contrast cardiovascular magnetic resonance for the measurement of diffuse myocardial fibrosis: preliminary validation in humans. *Circulation*. 2010;122:138–144.
9. Donahue KM, Burstein D, Manning WJ, Gray ML. Studies of Gd-DTPA relaxivity and proton exchange rates in tissue. *Magn Reson Med*. 1994;32:66–76.

10. Donahue KM, Weisskoff RM, Burstein D. Water diffusion and exchange as they influence contrast enhancement. *J Magn Reson Imaging*. 1997;7:102–110.
11. Landis CS, Li X, Telang FW, Molina PE, Palyka I, Vetek G, Springer CS Jr. Equilibrium transcytolemmal water-exchange kinetics in skeletal muscle in vivo. *Magn Reson Med*. 1999;42:467–478.
12. Jerosch-Herold M, Sheridan DC, Kushner JD, Nauman D, Burgess D, Dutton D, Alharethi R, Li D, Hershberger RE. Cardiac magnetic resonance imaging of myocardial contrast uptake and blood flow in patients affected with idiopathic or familial dilated cardiomyopathy. *Am J Physiol Heart Circ Physiol*. 2008;295:H1234–H1242.
13. Broberg CS, Chugh S, Peters D, Conklin C, Weiss J, Pantely GA, Sahn DJ, Jerosch-Herold M. Quantified diffuse myocardial fibrosis is associated with myocardial dysfunction in congenital heart disease. *Journal of the American College of Cardiology*. 2009;53:A364–A364.
14. Schelbert EB, Testa SM, Meier CG, Ceyrolles WJ, Levenson JE, Blair AJ, Kellman P, Jones BL, Ludwig DR, Schwartzman D, Shroff SG, Wong TC. Myocardial extravascular extracellular volume fraction measurement by gadolinium cardiovascular magnetic resonance in humans: slow infusion versus bolus. *J Cardiovasc Magn Reson*. 2011;13:16.
15. Feng M, Whitesall S, Zhang Y, Beibel M, D'Alecy L, DiPetrillo K. Validation of volume-pressure recording tail-cuff blood pressure measurements. *Am J Hypertens*. 2008;21:1288–1291.
16. Landis CS, Li X, Telang FW, Coderre JA, Micca PL, Rooney WD, Latour LL, Vétek G, Pâlyka I, Springer CS Jr. Determination of the MRI contrast agent concentration time course *in vivo* following bolus injection: effect of equilibrium transcytolemmal water exchange. *Magn Reson Med*. 2000;44:563–574.
17. Arnal JF, el Amrani AI, Chatellier G, Ménard J, Michel JB. Cardiac weight in hypertension induced by nitric oxide synthase blockade. *Hypertension*. 1993;22:380–387.
18. Pechánová O, Bernátová I, Pelouch V, Babál P. L-NAME-induced protein remodeling and fibrosis in the rat heart. *Physiol Res*. 1999;48:353–362.
19. Moreno H Jr, Metze K, Bento AC, Antunes E, Zatz R, de Nucci G. Chronic nitric oxide inhibition as a model of hypertensive heart muscle disease. *Basic Res Cardiol*. 1996;91:248–255.
20. Salton CJ, Chuang ML, O'Donnell CJ, Kupka MJ, Larson MG, Kissinger KV, Edelman RR, Levy D, Manning WJ. Gender differences and normal left ventricular anatomy in an adult population free of hypertension. A cardiovascular magnetic resonance study of the Framingham Heart Study Offspring cohort. *J Am Coll Cardiol*. 2002;39:1055–1060.
21. Messroghli DR, Nordmeyer S, Dietrich T, Dirsch O, Kaschina E, Savvatis K, Oh-Ici D, Klein C, Berger F, Kuehne T. Assessment of diffuse myocardial fibrosis in rats using small-animal Look-Locker inversion recovery T1 mapping. *Circ Cardiovasc Imaging*. 2011;4:636–640.
22. Li X, Springer CS Jr, Jerosch-Herold M. First-pass dynamic contrast-enhanced MRI with extravasating contrast reagent: evidence for human myocardial capillary recruitment in adenosine-induced hyperemia. *NMR Biomed*. 2009;22:148–157.
23. Seland JG, Bruvold M, Anthonsen H, Brurok H, Nordhøy W, Jynge P, Krane J. Determination of water compartments in rat myocardium using combined D-T1 and T1-T2 experiments. *Magn Reson Imaging*. 2005;23:353–354.
24. Donahue KM, Burstein D, Manning WJ, Gray ML. Studies of gd-dtpa relaxivity and proton exchange rates in tissue. *Magn Reson Med*. 1994;32:66–76.
25. Olivetti G, Giordano G, Corradi D, Melissari M, Lagrasta C, Gambert SR, Anversa P. Gender differences and aging: effects on the human heart. *J Am Coll Cardiol*. 1995;26:1068–1079.
26. Eisele JC, Schaefer IM, Randel Nyengaard J, Post H, Liebetanz D, Brüel A, Mühlfeld C. Effect of voluntary exercise on number and volume of cardiomyocytes and their mitochondria in the mouse left ventricle. *Basic Res Cardiol*. 2008;103:12–21.

CLINICAL PERSPECTIVE

Myocardial T1 measurements or mapping with cardiac magnetic resonance has been gaining increased attention as a valuable complement to late gadolinium enhancement imaging to assess pathological changes in the myocardium in the absence of late gadolinium enhancement. Diffuse fibrosis (and collagen deposition) is associated in several myocardial pathologies with an expansion of myocardial extracellular space. T1 measurements performed before and after injection of an extracellular contrast agent have been used to quantify the extracellular volume (ECV) fraction in myocardial tissue. As the expansion of the extracellular space with the build-up of diffuse fibrosis can be relatively small (≈10%), it is important to evaluate the limits of current approaches and determine the conditions for an accurate determination of ECV. We show that the estimation of ECV can be sensitive to water-exchange across cell-membranes, and more so when the ECV is expanded, and in the presence of ventricular hypertrophy, using a mouse model of hypertensive heart disease. Neglecting this effect, or assuming that water exchange is sufficiently fast even when contrast uptake creates large T1 differences between intra- and extracellular spaces leads to underestimation of ECV. The potential clinical relevance is tested in a small cohort of patients with hypertension. The findings of this study could help to better define conditions when relatively straightforward T1 measurements can give accurate estimates of ECV in patients.

Quantification of Cardiomyocyte Hypertrophy by Cardiac Magnetic Resonance: Implications on Early Cardiac Remodeling

Otavio R Coelho-Filho MD MPH[1,4*], Ravi V Shah MD[1*], Richard Mitchell MD PhD[3], Tomas G Neilan MD[1], Heitor Moreno Jr MD PhD[4], Bridget Simonson PhD[5], Raymond Kwong MD MPH[1], Anthony Rosenzweig MD[5], Saumya Das MD PhD[5], Michael Jerosch-Herold PhD[2]

[1]Cardiovascular Division, Department of Medicine, Brigham and Women's Hospital, Harvard Medical School, Boston, MA 02114;

[2]Department of Radiology, Brigham and Women's Hospital;

[3]Department of Pathology, Brigham and Women's Hospital;

[4]Department of Internal Medicine, State University of Campinas (Unicamp);

[5]Cardiovascular Institute, Beth Israel Deaconess Medical Center, Harvard Medical School, Boston, MA

*Drs. Coelho-Filho and Shah contributed equally to this work.

Running Title: Coelho-Filho and Shah—Cardiomyocyte Hypertrophy by MRI

Word Count: 6150 **(**Abstract word count: 250)

Correspondence to:

Michael Jerosch-Herold PhD

Associated Professor, Director of Cardiac Imaging Physics

Department of Radiology/Brigham and Women's Hospital

75 Francis Street, Radiology BWH Box #22

Boston, MA 02115

Tel: (617) 525-8959

Fax: (617) 264-5245

e-mail: mjeroch-herold@partners.org

ABSTRACT

Background: Cardiomyocyte hypertrophy is a critical precursor to the development of heart failure. Methods to phenotype cellular hypertrophy non-invasively are limited. The goal was to validate a CMR-based approach for the combined assessment of extracellular matrix expansion and cardiomyocyte hypertrophy.

Methods: Two murine models of pressure-overload, hypertension induced by L-NG-Nitroarginine Methyl Ester (L-NAME) and transaortic constriction (TAC), were imaged by CMR at baseline and 7-weeks after L-NAME treatment, and up to 7 weeks following TAC. T1 relaxation times were measured before and after gadolinium contrast. The intracellular lifetime of water (τ_{ic}), a cell size dependent parameter, and extracellular volume fraction (ECV), a parameter linked to interstitial connective tissue, were determined with a model for transcytolemmal water exchange. Minor (D_{min}) and major (D_{maj}) cell-diameters were measured on FITC-wheat germ agglutinin stained sections.

Results: $\tau_{ic,}$ correlated strongly with histologic cardiomyocyte volume-to-surface ratio (r=0.78, *P*<0.001) and cell volume (r=0.75; *P*<0.001). Histological cardiomyocyte diameters and cell volume were higher in mice treated with L-NAME for 7 weeks compared to controls (*P*<0.001). In the TAC model, there was an early increase in cell volume and cardiomyocyte size using both CMR and histology without early fibrosis. Mice exposed to TAC demonstrated a significant, longitudinal, and parallel increase in histological cell volume, volume-to-surface ratio, and $\tau_{ic,}$ between 2 and 7 weeks after TAC.

Conclusion: The intracellular lifetime (τ_{ic}) measured by contrast-enhanced CMR is a sensitive, non-invasive measure of cardiomyocyte hypertrophy that can longitudinally track hypertrophy and myocardial remodeling.

INTRODUCTION

Cardiomyocyte hypertrophy is an early response of the heart to stress, preceding left ventricular hypertrophy (LVH) and overt clinical heart failure (HF). Clinically, cardiomyocyte hypertrophy represents a conserved, plastic, and prognostically important response to a variety of physiologic (e.g., exercise) and pathophysiologic triggers (e.g., hypertension, aortic stenosis).[1-3] Although pathologic LVH may be reversible, the presence of LVH already confers a significantly higher risk of stroke, incident HF and mortality,[4-7] and accelerates the transition to HF.[8] Therefore, methods to detect and more precisely phenotype hypertrophy at the level of the cardiomyocyte may facilitate earlier detection and intervention, and potentially facilitate preventative therapy for HF.

In animal models, an increase in cardiomyocyte volume is an early marker of remodeling, occurring in response to mechanical stretch during the transition to HF.[9-11] At a macroscopic level, increased LV thickness is a manifestation of cardiomyocyte hypertrophy, as well as expansion of the extracellular matrix,[12] both of which play an integral role in the transition from compensated cardiac hypertrophy to clinical HF.[13] Despite the significance of cardiomyocyte hypertrophy to pathological molecular signaling in the heart, the lack of methods to serially quantify changes in cardiomyocyte volume *in vivo* with either therapy or varying physiologic conditions has limited the value of cardiomyocyte hypertrophy as a reversible target biomarker of preclinical disease.

The goal of this study was to establish and validate a novel cardiac magnetic resonance (CMR) technique to quantify cardiomyocyte hypertrophy at a cellular level, based on the concept that the lifetime of water within a cell changes with cell-size or cell-volume. We used two well-validated murine models of pressure-overload HF (hypertension and transverse aortic constriction) to validate the technique and establish its suitability for tracking longitudinal changes in cellular hypertrophy *in-vivo*.

METHODS

Murine model of hypertensive heart disease via L-nitro-w-methyl ester (L-NAME)

As a model of hypertensive heart disease, we studied mice treated with L-NAME, a well-described model in which myocardial fibrosis, hypertrophy, and failure occur simultaneously.[14-16] Thirty-three male wild-type mice (mean body weight 37.4±2.3 grams (Taconic, Germantown, NY, USA) were randomly assigned to one of two experimental groups: **1)** placebo (control group; n=15; tap water alone for 7 weeks) versus **2)** L-NAME-treated (L-NAME group; n=18; L-NAME 3mg/ml in drinking water; Sigma, USA) for 7 weeks. Animals were kept under standard conditions and had normal food and water ad *libitum*. Non-invasive tail blood pressures were obtained at baseline and weekly after treatment started, using a volume-pressure recording tail-cuff technique (CODA-1, Kent Scientific, Torrington, CT).[13] Mice in the control (placebo) and L-NAME groups were imaged at baseline and after 7 weeks of treatment (placebo versus L-NAME) using a 4.7T MRI system (Bruker Biospin MRI, Billerica, MA). Blood samples were collected by retro-orbital puncture immediately after each CMR study for blood hematocrit determination (i-STAT, Abbott Point-of-Care, Princeton, NJ). Mice treated with L-NAME, or placebo, were euthanized following the second CMR study. Hearts were excised and fixed in formalin-solution for histological analysis.

Murine model of pressure overload by transverse aortic constriction

Eleven mice (mean body weight 26.9±2.4 g, C57BL/6, Jackson Laboratory, Bar Harbor, Maine, USA) were subjected to transverse aortic constriction (TAC) at 3 months of age, as previously described.[17]. Mice were anesthetized with a ketamine/xylazine mix (80-100 mg/kg/12 mg/kg) and a thoracotomy was performed. The exposed transverse aortic arch was then ligated with a 27-gauge needle between the innominate artery and left common carotid

artery. Two weeks after surgery, mice underwent CMR (mean body weight 25.5±1.6 g, n=11) to assess early development of cardiomyocyte hypertrophy. To investigate longitudinal changes in hypertrophy and fibrosis, a subgroup of mice were imaged at 4 weeks (n=2) and 7 weeks (n=4) post TAC. Animals were imaged in a 9.8T MRI system (Bruker Biospin MRI, Billerica, MA). Blood sampling and euthanasia were performed at 2 weeks (n=5), 4 week (n=2) and 7 weeks (n=4).

Our study protocol and animal care conformed with the Guide for the Care and Use of Laboratory Animals, published by the National Institutes of Health (NIH Publication Number 85-23, Revised 1996), and was approved by the Standing Committee on Animal Care and Use at Harvard Medical School.

Histopathologic analysis

Heart tissues were fixed with buffered 10% formalin solution (Fisher Scientific, Pittsburgh, PA). Short axis sections (approximately 1mm thickness) of formalin-fixed tissue were processed and embedded in paraffin. To quantify cardiomyocyte size, sections were stained with fluorescein isothiocyanate-conjugated (FITC-) wheat germ agglutinin to delineate the cell membrane.[18] All sections were scanned with ScanScope scanners (Aperio Technologies, Inc; Vista, CA), and whole-slide images were sampled to a final resolution of 1.0μm/pixel. Ten measurements of minor (D_{min}) and major (D_{maj}) cell-diameters were obtained by image analysis of FITC-wheat germ agglutinin stained sections in the anterior wall, septal wall, lateral wall and inferior wall of each animal. For measurement of the major cell diameter in fields with longitudinally oriented myocytes, we selected only cells with well-defined cell membranes, and clearly visible cell nuclei. Cardiomyocyte volume was calculated assuming a cell shape in the form of a prolate ellipsoid,[19-22] using the median D_{min} and D_{maj} (see Figure 2). Connective tissue volume fraction was quantified on sections stained with Masson's trichrome stain, using a semi-automatic pixel color intensity algorithm in the Aperio Spectrum software to quantify pixels stained in blue.

Cardiac magnetic resonance imaging

Mice anesthetized with isofluorance (induction 4-5%; maintenance 1-2.5% in oxygen from a precision vaporizer) were positioned supine on a water-heated bed. CMR images were acquired with electrocardiographic and respiratory gating (model 1025L, SAII, Stony Brook, NY). For left ventricular (LV) size and function, short-axis cine gradient-echo images were acquired with full LV coverage (repetition time TR 5.9ms; echo time TE 2.2ms; temporal resolution 20-30ms; in-plane spatial resolution 100-120µm x 180-210µm; 1mm slice thickness, no gap). Manually traced epicardial and endocardial borders of matching short-axis cine locations at end-systole and end-diastole were used to determine the LV end-diastolic volume, LV end-systolic volume, and LV myocardial mass, using Simpson's rule, and LV ejection fraction (LVEF).

Gadolinium diethylenetriamine pentacetic acid (Magnevist, Berlex, Wayne, NJ) was injected subcutaneously in multiple steps up to a cumulative dose of 0.5mmol/kg. Myocardial T1 was measured in a mid-LV slice, once pre-contrast, and at least 4 times post-contrast, using a Look-Locker technique, no earlier than 6 minutes after contrast administration as described previously[23] (TR 2.5ms; TE 1.8ms; flip angle = 10°, in-plane resolution 190µm, 1mm slice thickness).

LV endocardial and epicardial borders were manually drawn. The signal intensity versus time curves for 6 myocardial segments and the blood pool were used to determine segmental T1 by non-linear least-squares fitting to an analytical expression for the magnitude signal measured during the inversion recovery, and correction for the radiofrequency pulse effects on the inversion recovery. The reciprocal of T1 (R1=1/T1) was used to plot the myocardial R1 against the R1 in the blood pool.

Determination of Intracellular Lifetime of Water

Water molecules exchange mostly by diffusion between the interstitial (extracellular) and intracellular spaces, with the average intracellular lifetime depending on the mean time for diffusion to the cell membrane (Figure 1). Specifically, the intracellular lifetime of water is proportional to the volume-to-surface ratio,[24,25] with the latter having a magnitude on the order of the *minor* cell diameter in the case of cardiomyocytes.

The myocardial T1 after administration of extra-cellular gadolinium contrast can be used to probe the intracellular lifetime of water.[24] The relaxation recovery rate (i.e. R1) of myocardial water changes linearly with the blood R1, as long as the rate of exchange of water between the extra- and intracellular spaces does not constitute a bottleneck (relative to the R1 difference between intra- and extra-cellular spaces). One moves away from this fast exchange regime, when the concentration of Gd-contrast in blood and the extracellular space is increased. The R1 of tissue then shows a sub-linear dependence on the R1 of blood.

The R1 for myocardial tissue and blood data were fit with a 2-space water-exchange (2SX) model of equilibrium transcytolemmal water-exchange, originally developed by Landis et al (Figure 2).[24,26] The myocardial extracellular volume fraction (ECV) and the intracellular lifetime of water are adjustable parameters of the model and determined by fitting the model to the observed R1 data with non-linear orthogonal distance regression algorithm. The measured blood hematocrit was a fixed parameter of the model.

An increase of intracellular lifetime of water (τ_{ic}), e.g. as result of increasing cell dimensions, increases the curvature in the relation between the R1 in myocardial tissue and the R1 of blood, which provides the basis for detecting cell-size changes. This is illustrated in Figure 1. Expansion of the myocardial interstitial space primarily affects the slope of the initially linear myocardial R1 curve, but has no direct effect on its curvature at higher R1 values.

Statistical Analyses

Continuous data were expressed as means ± standard deviation. Continuous variables were compared between groups of animals (e.g. L-NAME vs. placebo) by independent *t*-test, applied at each time point (baseline and 7-weeks) without adjustment of *P*-values. A paired *t*-test was used to compare measurements at baseline and follow-up within groups. Paired t-tests were performed for multiple measurement quantities (e.g. intracellular lifetime and ECV). Histograms for major and minor cell diameter measurements were used to estimate the empirical density distribution function over a grid of points, using the function *density* in the R statistical analysis environment. Correlations were assessed by Pearson's product moment correlation coefficient. For mice undergoing TAC, a non-paired *t*-test was used to compare baseline control mice with mice at 2 weeks after TAC. Longitudinal changes of τ_{ic} and ECV were analyzed with linear mixed-effects regression models. The *P*-values for the fixed effects in the linear mixed-effects models were calculated by Markov chain Monte Carlo sampling. Analyses were performed using SAS 9.3 (SAS Institute, Cary, NC) or R (version 2.15.1, R Foundation for Statistical Computing, Vienna, Austria; http://www.R-project.org/).

RESULTS

L-NAME and TAC induce significant LV hypertrophy

At baseline, control and L-NAME groups did not show any significant differences in body weight, blood pressure, heart rate, or CMR indices of LV structure and function (Table 1). Consistent with prior reports,[14-16] the chronic administration of L-NAME led to a significant increase in the mean blood pressure (88.1±7.4mmHg at baseline to 126.7±6.2mmHg at follow-up, $P<0.001$). After 7 weeks of treatment, the L-NAME and placebo-treated mice showed significant differences: LV mass increased in the L-NAME group (96.0±14.2mg vs.

163.9±21.6mg, *P*<0.001; *P*<0.001 when indexed to body weight), and a systolic function decreased (LVEF=60.8±3.1% vs. 50.1±7.7%, *P*<0.001). TAC mice developed significant and sustained LV hypertrophy after TAC (120.5±11.7mg at 2 weeks of TAC, and 147.8±8.2 at 7 weeks of TAC, *P*<0.0001 for unpaired comparisons with control group at baseline). TAC was also associated with a significant decrease in LVEF early after TAC (all *P*<0.0001 vs. control mice, Table 2). Effects on LV mass, LVEF, and LV volumes seen at 2 weeks after TAC were sustained at the 7 week post-TAC time point.

Interstitial fibrosis and extra-cellular space expansion in L-NAME and TAC models

After 7 weeks of L-NAME treatment, the histologically-measured connective tissue fraction was significantly higher than in placebo-treated mice (8.5±1.6% vs. 2.6±0.6%, *P*<0.001). In parallel, the myocardial ECV measured by CMR was also significantly higher for L-NAME versus placebo (0.42±0.08 vs, 0.25±0.03, *P*<0.001). Although mice exposed to TAC showed a significant increase in LV mass, they did not exhibit as marked an increase in histologic connective tissue fraction (2.3±0.1% for TAC at 7 weeks vs. 8.5±1.6% for L-NAME treated, *P*<0.001), or myocardial ECV (0.30±0.04 for TAC at 7 weeks vs. 0.42±0.08 for L-NAME, *P*=0.01) by 7 weeks (Table 2 and Figure 4).

Histologic assessment of cardiomyocyte hypertrophy

We measured the major (D_{maj}) and minor (D_{min}) cardiomyocyte dimensions and calculated cardiomyocyte volume, assuming a cell shape in the form of prolate ellipsoid (Figures 1 and 2).[19-22] L-NAME induced significant changes of D_{maj} (P<0.001 vs. placebo), averaging 7%, and a mean 32% change for D_{min} (*P*<0.001 vs. placebo; Table 1). The cardiomyocyte volume was 84% higher in mice treated with L-NAME versus placebo (78.09±12.86 10^4 x μmm^3 for L-NAME

treated mice and 42.34±6.01 10^4 x μmm^3 for placebo, P<0.001). The volume-to-surface ratio was also higher in L-NAME vs. placebo-treated mice (Table 1). The mice exposed to TAC had a significantly higher D_{min} compared to controls, with D_{min} reaching values similar to L-NAME treated mice (Table 2).

In a combined analysis of data from all experimental groups, D_{min}, but not D_{maj}, was significantly different after treatment in both TAC and L-NAME mice (Figure 3; P<0.001 for both TAC and L-NAME after 7 weeks as compared to control). Cardiomyocyte volume was significantly higher with longer exposure to TAC (56.66±7.39 10^4 x μmm^3 for 2 weeks of TAC exposure, and 73.42±2.53 10^4 x μmm^3 for 7 weeks, P=0.006), driven mostly by changes in D_{min}.

Intracellular lifetime of water as a marker of cardiomyocyte hypetrophy

The intracellular lifetime (τ_{ic}) of water, determined by CMR, was significantly higher after 7 weeks of L-NAME, compared to placebo treatment (0.19±0.07 vs. 0.44±0.12, P<0.001; Table 1, Figure 4). In the TAC-group, τ_{ic} increased significantly between 2 and 7 weeks after exposure to TAC (Table 2, and Figure 5). The rate of change of τ_{ic} with time after TAC surgery was estimated to be 0.0581 s/week (P<0.002), using a linear mixed effects model for the repeated measurements of τ_{ic} ranging from 2, to approximately 7 weeks post TAC. There was no significant difference τ_{ic} in mice after 7 weeks of L-NAME versus mice after 7 weeks of TAC (P=0.58).

When pooling all τ_{ic} values from CMR with time-matched histologic data, τ_{ic} demonstrated a strong positive association with cardiomyocyte volume-to-surface ratio (r=0.78, P<0.001; Figure 6). The correlation of τ_{ic} with cell-volume was r=0.75 (P<0.001), with median minor cell diameter r=0.79 (P<0.001), and with the median major cell diameter r=0.43 (P=0.006). τ_{ic} also demonstrated an inverse association with LVEF (r=-0.36 P=0.002).

DISCUSSION

This study validates a novel T1-based CMR technique to detect and quantify changes in cardiomyocyte hypertrophy. Serial measurements of τ_{ic} and myocardial ECV allowed the non-invasive identification of distinct but complementary aspects of myocardial remodeling at the cellular level. Specifically, the intracellular lifetime of water τ_{ic} was strongly associated with the histological volume-to-surface ratio, a measure of the characteristic cell size, as well as cardiomyocyte volume, and minor cell diameter. Not unexpectedly, the correlation of τ_{ic} with the major cell diameter was much weaker, and this parameter was also not well-suited to differentiate between normal and hypertrophied cardiomyocytes on histology. Our results suggest that development of interstitial fibrosis and cardiomyocyte hypertrophy can be temporally distinct and followed non-invasively. This is the first demonstration of the ability to track cardiomyocyte hypertrophy in-vivo non-invasively. It could be used in conjunction with more established applications of T1 mapping by CMR to facilitate earlier detection of pathologic hypertrophy and assess myocardial remodeling in response to therapeutic interventions.

Post-contrast T1 relaxation time measurements have been used in both animals [27, 28] and patients [29] with hypertension as an index of pathologic diffuse interstitial expansion. In prior work in aortic stenosis (1 - myocardial ECV fraction) was reported as an index of cell volume fraction.[30] It represents a combination of cell volume and density, rather than a direct measure of cellular hypertrophy. Our results suggest that myocardial interstitial expansion (e.g., myocardial ECV) and cardiomyocyte hypertrophy represent distinct characteristics of tissue structure, which can be measured serially by CMR.

From a biological perspective, increases in cardiac mass can result from interstitial matrix expansion (e.g., fibrosis or aberrant protein deposition) and/or increases in cardiomyocyte volume[31]. A differentiation between “physiologic” hypertrophy from “pathologic” hypertrophy may therefore require characterization of not only wall thickness and LV mass, but more specifically

interstitial matrix expansion and cardiomyocyte cell size directly. In states of pathologic hypertrophy in response to pressure overload, an increase in cardiomyocyte cell size has been considered an early and conserved hallmark, putatively occurring before the onset of irreversible myocardial fibrosis and subsequent ventricular dysfunction, remodeling, and HF.[9-11] In fact, mechanical stress has been associated with activation of a pro-fibrotic, pro-hypertrophic genetic program that may reinforce subsequent HF.[32-35] In turn, increases in interstitial fibrosis appear to mark the transition from compensated cellular and organ-level pathologic hypertrophy to HF.[9,36,37] In patients with LVH at risk for HF, alterations in the balance of collagen metabolism (as reflected by increases in matrix metalloproteinases and pro-collagen fragments) identify patients with clinical HF.[38-40] Early intervention at this stage, prior to development of overt fibrosis and myocardial dysfunction, may ameliorate the progression to overt HF.[41]

The proposed method has potential limitations: It is assumed that the cytolemmal permeability coefficient remains constant with the development of cell hypertrophy. Ischemic conditions could alter cell membrane permeability,[42] though it is unlikely that ischemia was a confounding factor in this study, based on the absence of apparent infarction by late-gadolinium enhancement.[42] Other cardiac resident cell types (e.g. fibroblasts) may bias or impair the detection of cardiomyocyte hypertrophy, but in viable myocardium the volume fraction of connective tissue, and the percentage of fibroblast volume is relatively small compared to the cardiomyocyte volume.

In conclusion, this study demonstrates and validates a non-invasive, T1-based CMR method for the assessment of cardiomyocyte hypertrophy. In models of pressure-overload HF, it was feasible to distinguish between cellular hypertrophy, characterizing the early tissue phenotype in TAC, and extracellular space expansion, a hallmark of chronic pressure overload. These results may help establish CMR as a non-invasive tool to quantify two critical aspects of early myocardial remodeling at the transition between compensated hypertrophy and clinical HF.

Acknowledgements

We would like to thank Deborah Burstein, PhD, director of the Beth Israel Deaconess Small Animal Imaging Facility, and Reza Akhavan, MS, for their support.

Sources of Funding

The Research reported in this publication was supported by the National Heart, Lung, and Blood Institute of the National Institutes of Health under Award Number R01HL090634. Drs. Coelho-Filho and Shah are supported by Post-Doctoral Fellowships from the American Heart Association (AHA 11POST5550053 to OCF and AHA 11POST110033 to RVS). Dr. Neilan is supported by an American Heart Association Fellow-to-Faculty grant (12FTF12060588).

REFERENCES

1. Devereux RB, Dahlof B, Levy D, Pfeffer MA. Comparison of enalapril versus nifedipine to decrease left ventricular hypertrophy in systemic hypertension (the preserve trial). The American journal of cardiology. 1996;78:61-65.

2. Dweck MR, Joshi S, Murigu T, Gulati A, Alpendurada F, Jabbour A, et al. Left ventricular remodelling and hypertrophy in patients with aortic stenosis: Insights from cardiovascular magnetic resonance. Journal of cardiovascular magnetic resonance: official journal of the Society for Cardiovascular Magnetic Resonance. 2012;14:50.

3. Sharma S, Maron BJ, Whyte G, Firoozi S, Elliott PM, McKenna WJ. Physiologic limits of left ventricular hypertrophy in elite junior athletes: Relevance to differential diagnosis of athlete's heart and hypertrophic cardiomyopathy. Journal of the American College of Cardiology. 2002;40:1431-1436.

4. Devereux RB, Dahlof B, Gerdts E, Boman K, Nieminen MS, Papademetriou V, et al. Regression of hypertensive left ventricular hypertrophy by losartan compared with atenolol: The losartan intervention for endpoint reduction in hypertension (life) trial. Circulation. 2004;110:1456-1462

5. Kannel WB, Gordon T, Offutt D. Left ventricular hypertrophy by electrocardiogram. Prevalence, incidence, and mortality in the framingham study. Annals of internal medicine. 1969;71:89-105.

6. Larstorp AC, Okin PM, Devereux RB, Olsen MH, Ibsen H, Dahlof B, et al. Regression of ecg-lvh is associated with lower risk of new-onset heart failure and mortality in patients with isolated systolic hypertension; the life study. American journal of hypertension. 2012.

7. Lindholm LH, Ibsen H, Dahlof B, Devereux RB, Beevers G, de Faire U, et al. Cardiovascular morbidity and mortality in patients with diabetes in the losartan intervention for endpoint reduction in hypertension study (life): A randomised trial against atenolol. Lancet. 2002;359:1004-1010.

8. Olivetti G, Melissari M, Balbi T, Quaini F, Cigola E, Sonnenblick EH, et al. Myocyte cellular hypertrophy is responsible for ventricular remodelling in the hypertrophied heart of middle aged individuals in the absence of cardiac failure. Cardiovasc Res. 1994;28:1199-1208.

9. Boluyt MO, O'Neill L, Meredith AL, Bing OH, Brooks WW, Conrad CH, et al. Alterations in cardiac gene expression during the transition from stable hypertrophy to heart failure. Marked upregulation of genes encoding extracellular matrix components. Circulation research. 1994;75:23-32

10. Lorell BH, Carabello BA. Left ventricular hypertrophy: Pathogenesis, detection, and prognosis. Circulation. 2000;102:470-479.

11. Scimia MC, Hurtado C, Ray S, Metzler S, Wei K, Wang J, et al. Apj acts as a dual receptor in cardiac hypertrophy. Nature. 2012.

12. de Simone G, de Divitiis O. Extracellular matrix and left ventricular mechanics in overload hypertrophy. Adv Clin Path. 2002;6:3-10.

13. Iwanaga Y, Aoyama T, Kihara Y, Onozawa Y, Yoneda T, Sasayama S. Excessive activation of matrix metalloproteinases coincides with left ventricular remodeling during transition from hypertrophy to heart failure in hypertensive rats. J Am Coll Cardiol. 2002;39:1384-1391.

14. Arnal JF, el Amrani AI, Chatellier G, Menard J, Michel JB. Cardiac weight in hypertension induced by nitric oxide synthase blockade. Hypertension. 1993;22:380-387.

15. Moreno HJr., Metze K, Bento AC, Antunes E, Zatz R, de Nucci G. Chronic nitric oxide inhibition as a model of hypertensive heart muscle disease. Basic Res Cardiol. 1996;91:248-255.

16. Pechanova O, Bernatova I, Pelouch V, Babal P. L-name-induced protein remodeling and fibrosis in the rat heart. Physiol Res. 1999;48:353-362.

17. Xiao CY, Chen M, Zsengeller Z, Li H, Kiss L, Kollai M, et al (adp-ribose) polymerase promotes cardiac remodeling, contractile failure, and translocation of apoptosis-inducing factor in a murine experimental model of aortic banding and heart failure. J Pharmacol Exp Ther. 2005;312:891-898.

18. Xu J, Kimball TR, Lorenz JN, Brown DA, Bauskin AR, Klevitsky R, et al. Gdf15/mic-1 functions as a protective and antihypertrophic factor released from the myocardium in association with smad protein activation. Circ Res. 2006;98:342-350.

19. Yaniv Y, Juhaszova M, Wang S, Fishbein KW, Zorov DB, Sollott SJ. Analysis of mitochondrial 3d-deformation in cardiomyocytes during active contraction reveals passive structural anisotropy of orthogonal short axes. PLoS One. 2011;6:e21985.

20. Thomas TA, Kuzman JA, Anderson BE, Andersen SM, Schlenker EH, Holder MS, et al. Thyroid hormones induce unique and potentially beneficial changes in cardiac myocyte shape in hypertensive rats near heart failure. Am J Physiol Heart Circ Physiol. 2005;288:H2118-2122.

21. Boyett MR, Frampton JE, Kirby MS. The length, width and volume of isolated rat and ferret ventricular myocytes during twitch contractions and changes in osmotic strength. Exp Physiol. 1991;76:259-270.

22. Sorenson AL, Tepper D, Sonnenblick EH, Robinson TF, Capasso JM. Size and shape of enzymatically isolated ventricular myocytes from rats and cardiomyopathic hamsters. Cardiovasc Res. 1985;19:793-799.

23. Coelho-Filho OR, Mongeon FP, Mitchell R, Moreno HJr., Nadruz WJr., Kwong R, et al. The role of transcytolemmal water exchange in magnetic resonance measurements of diffuse myocardial fibrosis in hypertensive heart disease. Circ Cardiovasc Imaging. 2012.

24. Landis CS, Li X, Telang FW, Molina PE, Palyka I, Vetek G, et al. Equilibrium transcytolemmal water-exchange kinetics in skeletal muscle in vivo. Magn Reson Med. 1999;42:467-478.

25. Yankeelov TE, Rooney WD, Huang W, Dyke JP, Li X, Tudorica A, et al. Evidence for shutter-speed variation in cr bolus-tracking studies of human pathology. NMR Biomed. 2005;18:173-185.

26. Landis CS, Li X, Telang FW, Coderre JA, Micca PL, Rooney WD, et al. Determination of the mri contrast agent concentration time course in vivo following bolus injection: Effect of equilibrium transcytolemmal water exchange. Magn Reson Med. 2000;44:563-574.

27. Messroghli DR, Nordmeyer S, Buehrer M, Kozerke S, Dietrich T, Kaschina E, et al. Small animal look-locker inversion recovery (salli) for simultaneous generation of cardiac t1 maps and cine and inversion recovery-prepared images at high heart rates: Initial experience. Radiology. 2011; 261:258-265.

28. Messroghli DR, Nordmeyer S, Dietrich T, Dirsch O, Kaschina E, Savvatis K, et al. Assessment of diffuse myocardial fibrosis in rats using small-animal look-locker inversion recovery t1 mapping. Circulation. Cardiovascular imaging. 2011;4:636-640.

29. Ugander M, Oki AJ, Hsu LY, Kellman P, Greiser A, Aletras AH, et al. Extracellular volume imaging by magnetic resonance imaging provides insights into overt and sub-clinical myocardial pathology. European heart journal. 2012;33:1268-1278.

30. Flett AS, Sado DM, Quarta G, Mirabel M, Pellerin D, Herrey AS, et al. Diffuse myocardial fibrosis in severe aortic stenosis: An equilibrium contrast cardiovascular magnetic resonance study. Eur Heart J Cardiovasc Imaging. 2012;13:819-826.

31. Dorn GW, Robbins J, Sugden PH. Phenotyping hypertrophy: Eschew obfuscation. Circulation research. 2003;92:1171-1175.

32. Adams JW, Sakata Y, Davis MG, Sah VP, Wang Y, Liggett SB, et al. Enhanced galphaq signaling: A common pathway mediates cardiac hypertrophy and apoptotic heart failure. Proceedings of the National Academy of Sciences of the United States of America. 1998;95:10140-10145.

33. Hein S, Arnon E, Kostin S, Schonburg M, Elsasser A, Polyakova V, et al. Progression from compensated hypertrophy to failure in the pressure-overloaded human heart: Structural deterioration and compensatory mechanisms. Circulation. 2003;107:984-991.

34. Krayenbuehl HP, Hess OM, Monrad ES, Schneider J, Mall G, Turina M. Left ventricular myocardial structure in aortic valve disease before, intermediate, and late after aortic valve replacement. Circulation. 1989;79:744-755.

35. Sanada S, Hakuno D, Higgins LJ, Schreiter ER, McKenzie AN, Lee RT. Il-33 and st2 comprise a critical biomechanically induced and cardioprotective signaling system. The Journal of clinical investigation. 2007;117:1538-1549.

36. Mohammed SF, Ohtani T, Korinek J, Lam CS, Larsen K, Simari RD, et al. Mineralocorticoid accelerates transition to heart failure with preserved ejection fraction via "nongenomic effects". Circulation. 2010;122:370-378.

37. Shapiro BP, Owan TE, Mohammed S, Kruger M, Linke WA, Burnett JCJr., Redfield MM. Mineralocorticoid signaling in transition to heart failure with normal ejection fraction. Hypertension. 2008;51:289-295.

38. Ahmed SH, Clark LL, Pennington WR, Webb CS, Bonnema DD, Leonardi AH, et al. Matrix metalloproteinases/tissue inhibitors of metalloproteinases: Relationship between changes in proteolytic determinants of matrix composition and structural, functional, and clinical manifestations of hypertensive heart disease. Circulation. 2006;113:2089-2096.

39. Martos R, Baugh J, Ledwidge M, O'Loughlin C, Murphy NF, Conlon C, et al. Diagnosis of heart failure with preserved ejection fraction: Improved accuracy with the use of markers of collagen turnover. European journal of heart failure. 2009;11:191-197.

40. Post WS, Larson MG, Myers RH, Galderisi M, Levy D. Heritability of left ventricular mass: The framingham heart study. Hypertension. 1997; 30:1025-1028.

41. Zannad F, McMurray JJ, Krum H, van Veldhuisen DJ, Swedberg K, Shi H, et al. Eplerenone in patients with systolic heart failure and mild symptoms. N Engl J Med. 2011;364:11-21.

42. Zhang Y, Poirier-Quinot M, Springer CSJr., Balschi JA. Active trans-plasma membrane water cycling in yeast is revealed by nmr. Biophys J. 2011; 101:2833-2842.

Table-1- Baseline and follow-up hemodynamic and CMR characteristics of control and L-NAME treated mice. Abbreviations: LVEF=left ventricular ejection fraction, LVEDV=left ventricular end-diastolic volume, LVESV=left ventricular end-systolic volume. Cell entries with a dash refer to histological measurements not available for baseline.

	Baseline			7-week		
Characteristics (hemodynamic and CMR data)	**Control (n=15)**	**L-NAME (n=18)**	***P*-value***	**Control (n=13)**	**L-NAME (n=17)**	***P*-value***
Body weight [g]	37.5±2.7	37.7±2.4	0.865	44.8±4.5$^{\&}$	40.0±3.2$^{\&}$	0.002
Heart rate [bpm]	492.1±108.0	499.7±73.5	0.827	403.1±94.3	474.1±69.7	0.410
Mean blood pressure [mmHg]	92.2±7.3	88.1±7.4	0.209	91.3±8.1	126.7±6.2$^{\&}$	<0.001
LVEF [%]	57.8±3.9	58.4±3.0	0.629	60.8±3.1	50.1±7.7$^{\$}$	<0.001
LVEDV [µl]	129.9±32.2	146.9±31.9	0.187	110.51±25.7	122.5±37.2$^{\&}$	0.228
LVESV [µl]	54.7±13.8	61.1±14.1	0.255	41.6±11.2$^{\&}$	60.6±19.6	0.009
LVmass [mg]	96.7±16.7	93.8±12.2	0.615	96.0±14.2	163.9±21.6$^{\&}$	<0.001
LV mass indexed to body weight [mg/g]	2.5±0.5	2.5±0.4	0.592	2.2±0.1$^{\&}$	4.1±0.5$^{\&}$	<0.001
Myocardial extracellular volume fraction (MRI)	0.26±0.02	0.27±0.03	0.677	0.25±0.03	0.42±0.08$^{\&}$	<0.001
Intracellular life time of water [1/s]	0.15±0.07	0.17±0.05	0.791	0.19±0.07	0.44±0.12$^{\&}$	<0.001
Connective tissue fraction (histology), %	-	-	-	2.6±0.6	8.5±1.6	<0.001
D_{maj} [µm; major cell diameter]	-	-	-	84.28±3.55	90.37±5.1	0.0012
D_{min} [µm; minor cell diameter]	-	-	-	19.81±0.94	26.15±1.59	<0.001
D_{maj} /D_{min}	-	-	-	4.26±0.22	3.46±0.15	<0.001
Cardiomyocyte volume by histology [10^4 x µm^3]	-	-	-	42.34±6.01	78.09±12.86	<0.001
Cell Surface Area [10^4 µm^2]	-	-	-	1.70±0.14	2.41±0.26	<0.001
Volume-to-Surface ratio (V/S) [µm]	-	-	-	24.66±1.44	32.24±1.91	<0.001

****P*-**values for unpaired t-test of control vs. L-NAME mice; $^{\&}$ *P*<0.05 for paired t-test of baseline vs. 7-week mice (control and L-NAME)

Table 2- Hemodynamic and CMR characteristics of control and TAC mice at time of first MRI post transaortic constriction. Abbreviations: LVEF=left ventricular ejection fraction, LVEDV=left ventricular end-diastolic volume, LVESV=left ventricular end-systolic volume, RVEF=right ventricular ejection fraction, RVEDV=right ventricular end-diastolic volume, RVESV=right ventricular end-systolic volume. Adjusted p-values refer to result of unpaired t-test for comparison of mice at 2 weeks post TAC surgery, to controls (Table 1). The adjusted *P*-values marked with *refer to comparisons with 12 week old mice in the control group

Characteristics (hemodynamic and CMR data)	**2 weeks (n=11)**	***P* -value**
LVEF [%]	36.8±6.3	<0.0001
LVEDV [µl]	91.5±24.4	<0.0001
LVESV [µl]	59.1±20.1	<0.0001
LV mass [mg]	120.5±11.7	<0.0001
LV mass indexed to body weight [mg/g]	4.7±0.3	<0.0001
Myocardial extracellular volume fraction	0.25±0.03	0.2681
Intracellular life time of water [1/s]	0.22±0.05	0.0181
D_{maj} [µm]	87.06±1.11	0.09*
D_{min} [µm]	22.81±1.43	0.02*
D_{maj}/D_{min}	3.83±0.24	0.09*
Connective tissue fraction (histology), %	2.3±0.1	<0.0001*
Cardiomyocyte volume by histology [10^4 x μm^3]	56.66±7.39	0.005*
Cell Surface Area [10^4 x μm^2]	2.01±0.15	0.01*
Volume-to-Surface ratio (V/S) [µm]	28.27±1.64	0.04*

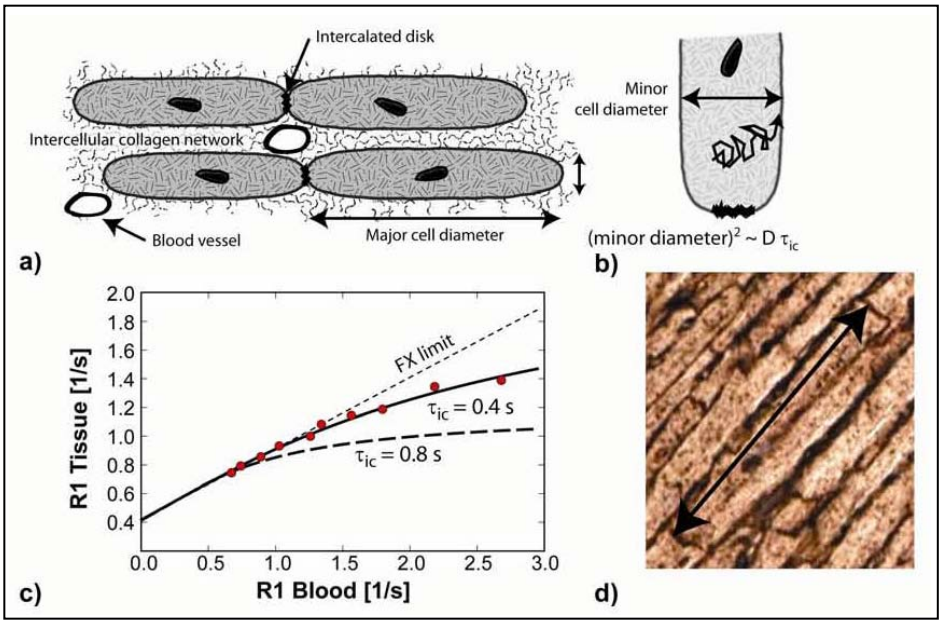

Figure 1- Illustration of cardiomyocyte hypertrophy determination. **(A)** Cardiomyocytes have an elongated shape with the ratio of the major-to-minor cell-diameter on the order of 4:1. **(B)** The intracellular lifetime (τ_{ic}) of a water molecule undergoing diffusional motion within the cell is proportional to the volume-to-surface ratio (V/S), a measure of cell size. **(C)** CMR measurements of the longitudinal relaxation rate constant (R1) before and after administration of gadolinium contrast were used to determine τ_{ic}. The relation between R1 in myocardial tissue and R1 of blood starts out linear, with a slope proportional to the extracellular volume fraction. With increasing R1 in blood, τ_{ic} ceases to be sufficiently short relative to the extra-to-intracellular R1 difference, and the degree of deviation from linear dependence is sensitive to τ_{ic}. Red data circles are from measurements in a mouse at 7 weeks after transverse aortic constriction. The solid line is the fit to the data with a two-space water-exchange model. The τ_{ic} for the best fit was 0.4s. The line with long dashes illustrates how the model fit changes with an increase of τ_{ic} to 0.8s, which causes a larger deviation from the straight line. **(D)** D_{maj} was measured on digitized images of tissue slices stained with fluorescein isothiocyanate-conjugated (FITC-) wheat germ agglutinin as the distance between the intercalated discs.

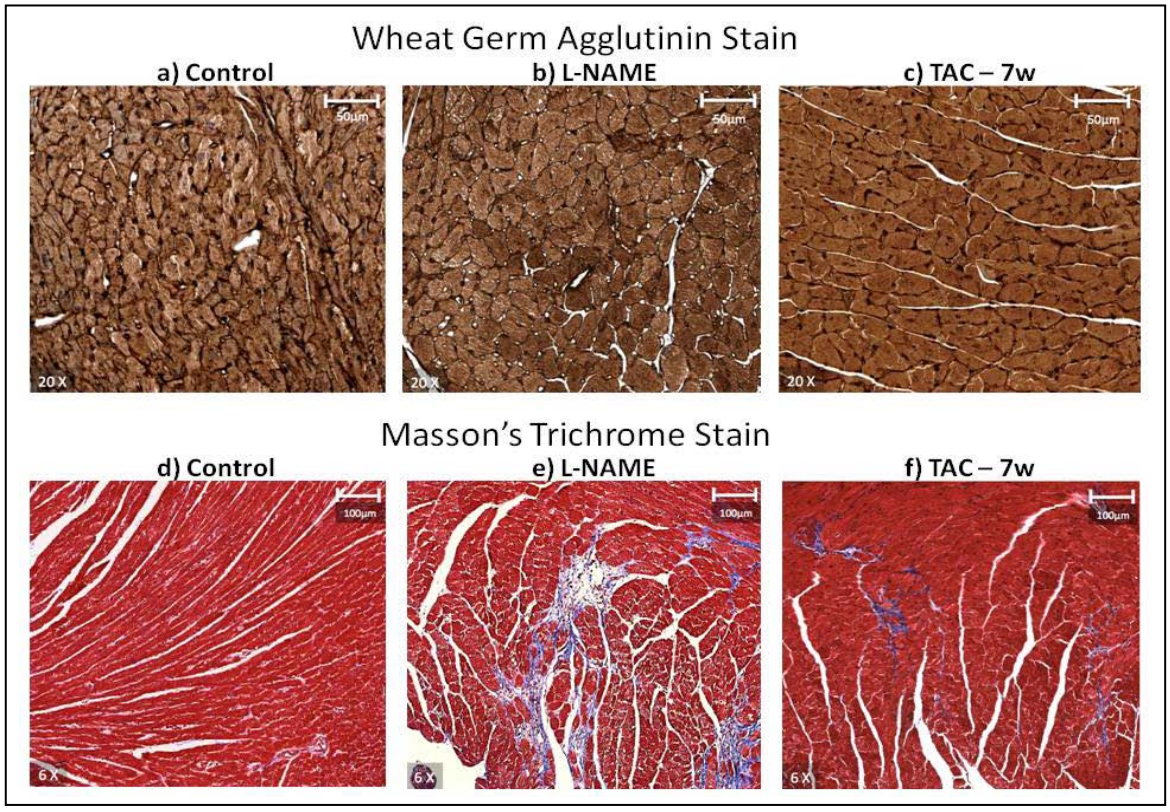

Figure 2- Cellular hypertrophy and interstitial fibrosis in L-NAME and TAC mice. Short-axis, mid-level LV sections of cardiac tissue from mice treated with placebo **(panel A)**, L-NAME **(panel B)**, and TAC **(panel C)**. L-NAME and TAC are representative tissues after 7 weeks of exposure. Panels were stained with fluorescein isothiocyanate-conjugated (FITC-) wheat germ agglutinin to delineate cell membranes and scanned at a resolution equivalent to 1.0µm/pixel to measure minor and major cell diameters in 15 fields within 4 myocardial segments. The images in **(A)-(B)** are representative illustrations of larger short-axis diameters in the L-NAME and TAC groups relative to controls. Adjacent short-axis sections from the same mice, stained with Masson's trichrome stains in **(D)-(F)** illustrate the absence of interstitial fibrosis in the control group and higher levels of interstitial fibrosis (blue) in L-NAME compared to TAC mice.

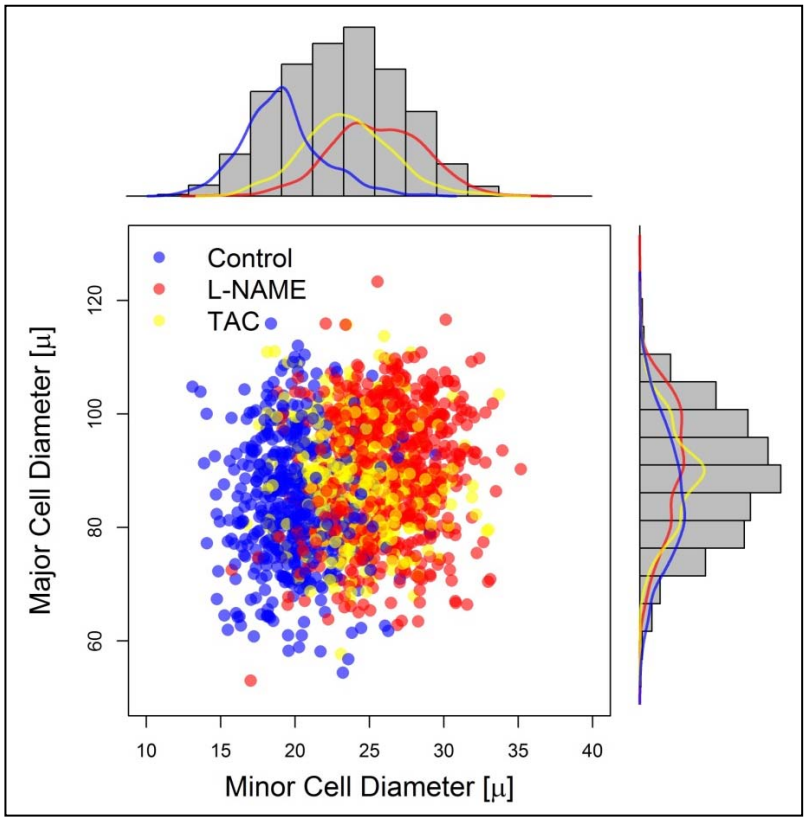

Figure 3- Relationship between major and minor cell diameters across L-NAME and TAC mice. Major cell diameters (D_{maj}, vertical axis) were plotted against minor cell diameters (D_{min}) for all three experimental groups (controls, L-NAME, and TAC mice) to assess which is better for discriminating between placebo, L-NAME and TAC groups. There were no significant differences in D_{maj} after L-NAME, placebo, or TAC (control: 84.28±3.55μm; L-NAME: 90.37±5.1μm; 7 week post TAC: 88.49±1.05μm), while D_{min} (control: 19.81±0.94μm; L-NAME: 26.15±1.59μm; 7 week post TAC: 25.85±0.89μm) varied significantly (P<0.001). This is also illustrated by the histograms for D_{min} (top) and D_{maj} (right side). The continuous lines in the histograms show kernel density estimates for each group. While these probability density estimates essentially overlap for the three experimental groups in the case of D_{maj}, the peaks of the density estimates for D_{min} are distinct.

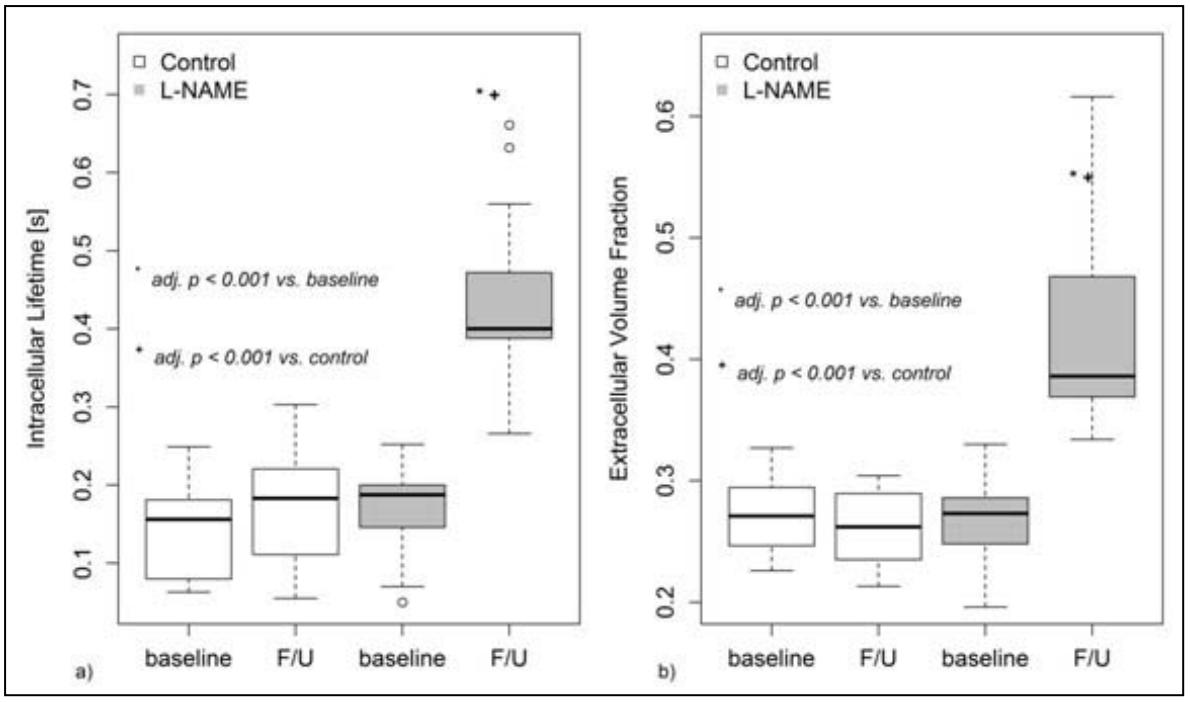

Figure 4- (A) The intracellular lifetime of water (τ_{ic}) increased significantly in mice treated with L-NAME, and was significantly higher than in placebo-treated controls. **(B)** In mice exposed for 7 weeks to L-NAME the extracellular volume fraction increased also significantly, compared to baseline, and was also significantly higher than in placebo-treated controls.

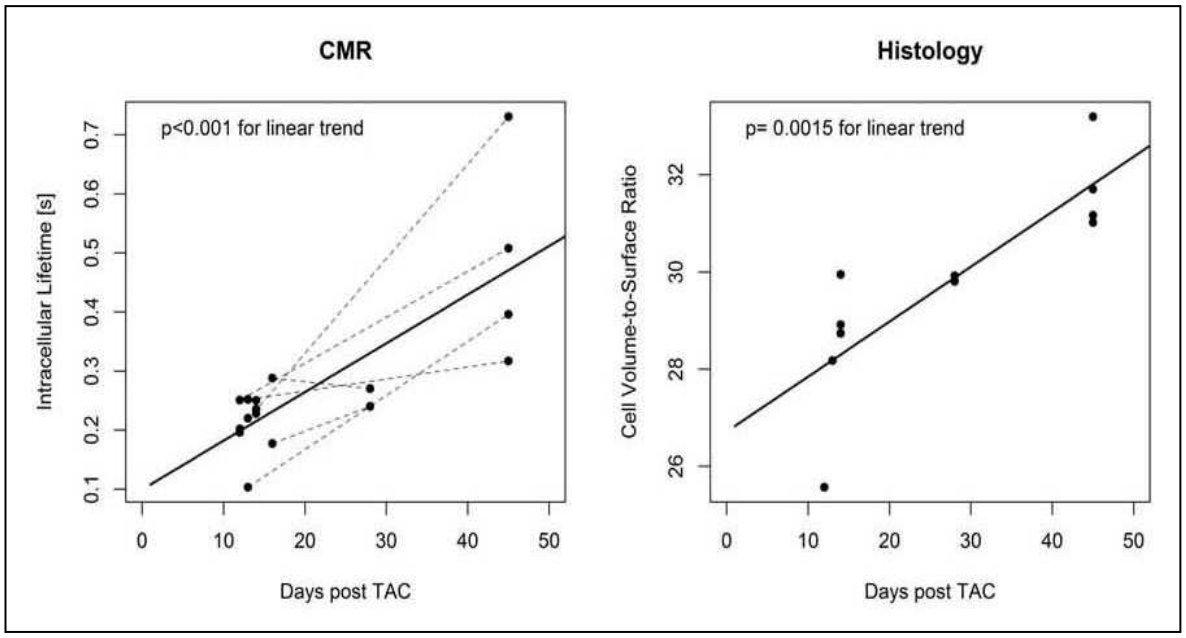

Figure 5- A) Mice were imaged at approximately 2 weeks after transaortic constriction, and followed-up for up to 46 days before harvesting of the heart. Over this time the intracellular lifetime increased significantly (0.0581 s/week; *P*=0.0002) as illustrated by the solid line, calculated with a linear mixed effects model. Dashed lines connect repeated measurements within the same mouse. **B)** The cell-volume-to-surface ratio calculated from the histologic major and minor cell diameters showed a significant association with the time between TAC and histological examination (0.79±0.18μm/week; *P*=0.001). The solid line represents the linear regression fit to the data.

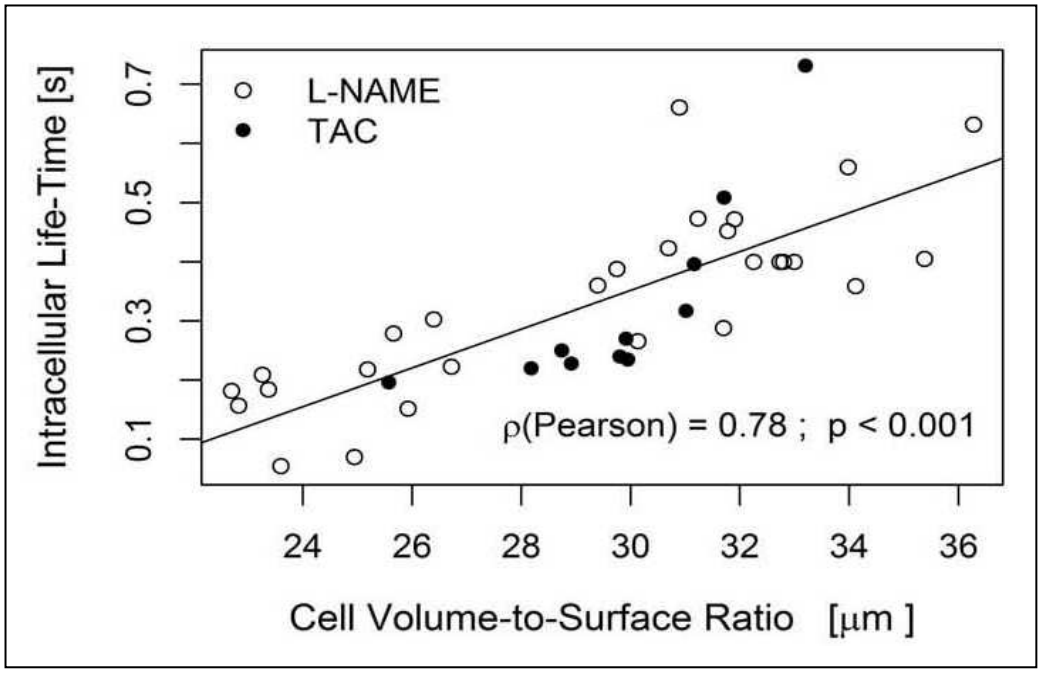

Figure 6- Association between intracellular lifetime of water and cell volume-to-surface ratio. For a diffusion-based exchange the intracellular lifetime of water is expected to be proportional to the cellular volume-to-surface ratio. The volume-to-surface ratio (V/S) was highly correlated (r=0.78; *P*<0.001) with the intracellular lifetime of water obtained from the water T1 measurements before and after administration of an extracellular gadolinium contrast agent.

4- DISCUSSÃO GERAL

O presente estudo apresenta os seguintes achados principais:

1- Medidas de T1 antes e depois da administração de um contraste extracelular, o gadolínio, detectou precisamente a expansão da matriz extracelular, em dois modelos animais de sobrecarga pressórica no coração (com a administração de L-NAME e com a bandagem da aorta), assim como em uma coorte de pacientes com hipertensão.

2- Caso o efeito da troca transmembrana de água seja negligenciado, a expansão da matriz extracelular e a hipertrofia miocárdica podem acentuar a subestimação da FVEC pelas medidas de T1 derivadas da RMC.

3- O TVIMA apresentou íntima correlação com a relação volume/superfície e volume dos cardiomiócitos.

4- A determinação da FVEC e do TVIMA através das medidas de T1 pela RMC antes e depois da administração de gadolínio-DTPA, permitiu caracterizar conjuntamente dois importantes componentes do remodelamento cardíaco: o espaço extracelular e a hipertrofia dos cardiomiócitos.

A expansão do espaço extracelular e a hipertrofia miocárdica são importantes fatores que influenciam a subestimação da FVEC, quando o efeito da troca transmembrana de água não é levada em consideração nas medidas de T1 pela RMC. Quando o modelo de 2 compartimentos é utilizado, que leva em consideração a troca de água pela membrana celular, as estimativas da FVEC apresentam excelente correlação com a medida histológica direta do tecido conectivo pela coloração de Tricrômico de Masson. Ao analisarmos as medidas de T1 antes e depois da administração de contraste gadolínio com o auxilio de um modelo de dois compartimentos, encontramos também na coorte de pacientes hipertensos aumento significativo da matriz extracelular não detectada pela massa do ventrículo esquerdo ou pelo realce tardio, ambos pela RMC. A magnitude do aumento da FVEC apresentou forte correlação com o volume atrial nos pacientes

hipertensos, o que corrobora o conceito que fibrose intersticial promove disfunção diastólica e aumento das pressões de esvaziamento do ventrículo esquerdo (82-84).

Parte desse estudo apresentou como objetivo validar que a medida do matriz extracelular pela RMC contra histologia. Estudos prévios validaram a medida da FVEC pela RMC contra histologia com coloração *picrosirius red* (70). *Picrosirius red* é uma coloração relativamente sensível para a identificação de colágeno, particularmente o colágeno do tipo I, através da visualização das laminas com uso de luz polarizada, que evidência a orientação das fibras de colágeno. Apesar disso, em condição com menor quantidade de fibrose intersticial, ou em estágios mais precoces de deposição do colágeno, quando predomina o acúmulo de glicosaminoglicanas, proteoglicanas, firbonectina e colágeno tipo III, a coloração *picosirius red* pode ser um método menos útil para avaliar a expansão da matriz extracelular (85). Dessa forma, nesse estudo optamos por utilizar a coloração de Tricrômico de Masson, para evidenciar e quantificar todos os componentes da expansão do espaço extracelular, incluindo componentes não relacionados diretamente ao colágeno, que estão presentes na doença cardíaca hipertensiva.

Nosso estudo confirmou que a troca transmembrana de água pode desempenhar um importante papel na determinação do tempo T1 no miocárdio, sobretudo quando um contraste extracelular, como o gadolínio, cria diferença nos valores de R1 entre o intracelular e o extracelular na mesma ordem da troca transmembrana de água. A inclusão do papel da troca transmembrana de água na quantificação da FVEC requer a utilização de um modelo de dois compartimentos, que já foi aplicado e validado para o músculo esquelético (76,86). O uso do modelo com dois compartimentos permite uma quantificação mais precisa da FVEC além da quantificação de uma outra variável, o TVIMA, através da quantificação do desvio da relação linear do R1 plasma com o R1 (Figura 3). O TVIMA reflete uma propriedade do tecido, sendo que não existem evidências que sofra influência com a administração do contraste gadolínio.

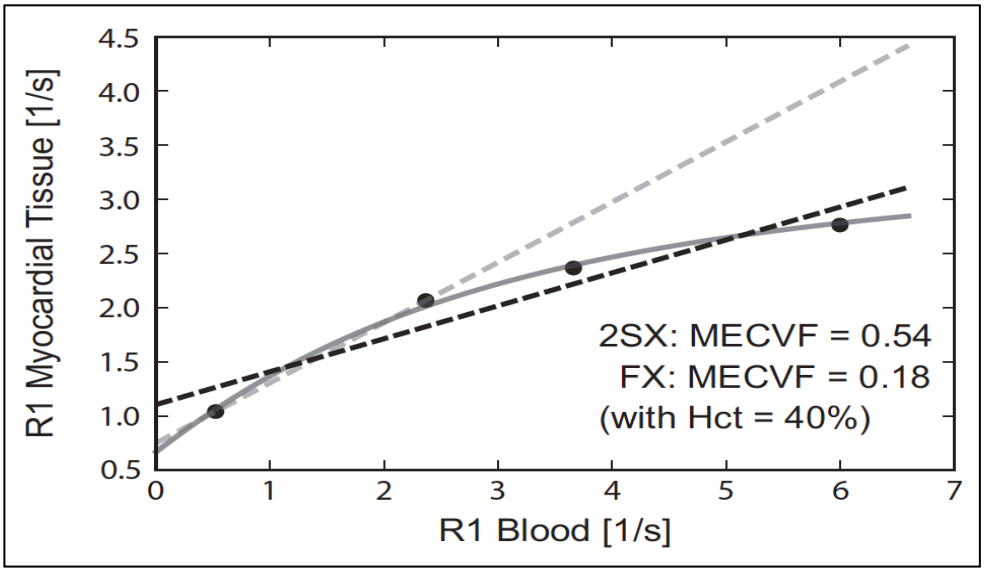

Figura 3- Papel da troca transmembrana de água na determinação da FEVC

Essa figura mostra a relação do R1 no miocárdio (eixo Y) com o R1 no plasma (eixo X). A linha tracejada em cinza refere-se ao modelo linear simples. A Linha sólida em cinza refere-se ao modelo com dois compartimentos.

O viés introduzido pelo uso do modelo linear simples, que não leva em conta a troca transmembrana de água, aumentou com o aumento da FVEC e com o aumento do TVIMA, sendo também dependente dos valores de R1 no plasma. A maior diferença entre o modelo linear e o modelo com dois compartimentos foi visto nos animais tratados com L-NAME, o que provavelmente reflete o desenvolvimento substancial de hipertrofia e fibrose intersticial.

Incluímos na coorte de pacientes clínicos desse estudo apenas indivíduos hipertensos com massa ventricular esquerda dentro da normalidade para a faixa etária e sexo. Apesar disso a FVEC foi significativamente maior quando comparada ao valor dos pacientes controles, sugerindo que a expansão da matriz extracelular ocorra antes do aumento significativo da massa ventricular esquerda. Essa última, a massa ventricular esquerda, parece ser influenciada não apenas pela expansão da matriz extracelular, mas também pela hipertrofia celular.

Terapias medicamentosas, como os inibidores da enzima de conversão, podem influenciar a regressão da hipertrofia ventricular esquerda (87), e assim se beneficiar de novos marcadores precoces de remodelamento cardíaco.

Toda a metodologia, incluindo a sequência de pulso utilizada e o pós-processamento, foi semelhante entre os estudos realizados em camundongos e humanos. Os estudos realizado nos camundongos, devido a menor dimensão dos animais, necessitou de melhor definição temporal e melhor definição espacial. Além disso, os camundongos foram estudados sob anestesia inalatória em equipamento de ressonância magnética dedicado para estudos em animais. No caso dos animais, a administração do contraste gadolínio foi feito por via subcutânea, e no caso dos estudos clínicos em humanos, foi administrado contraste por acesso venoso periférico. Apesar dessas mínimas diferenças técnicas, o efeito da troca transmembrana da água na determinação da FVEC foi semelhante entre os estudos realizados nos camundongos e nos pacientes, ainda que nesses últimos foi utilizada dose de gadolínio aceita clinicamente de 0,15mmol/kg.

Nós mostramos que a expansão da matriz extracelular e da hipertrofia miocárdica podem exacerbar a subestimação da FVEC, caso a troca de água pela membrana celular nas medidas de T1 pela RMC seja negligenciado. Essa nova maneira de se analisar as medidas de T1 pela RMC antes a após a administração de contraste gadolínio, utilizando um modelo de 2 compartimentos (76), nos permitiu obter um novo parâmetro diretamente relacionada com o tamanho e volume dos cardiomiócitos.

A partir desse novo conceito, desenvolvemos e validamos a quantificação do tempo intracelular da água como um marcador de hipertrofia de cardiomiócitos. Dessa forma esse estudo também validou um método derivado de medidas de T1 pela RMC, para detectar além da expansão da matriz extracelular, a hipertrofia de cardiomiócitos em dois modelos distintos de sobrecarga pressórica no coração (L-NAME e bandagem da aorta). Medidas seriadas do TVIMA e FVEC permitiram a identificação de diferentes padrões de remodelamento no miocárdico.

Especificamente, o TVIMA apresentou robusta associação com a relação volume/superfície celular, uma medida característica do tamanho celular. TVIMA também apresentou íntima correlação com o volume celular e com diâmetro menor dos cardiomiócitos. Não obstante, a correlação entre TVIMA com o diâmetro maior foi muito mais fraca que a associação com diâmetro menor dos cardiomiócitos. Da mesma maneira a o diâmetro maior pela histologia não diferenciou adequadamente os cardiomiócitos normais dos hipertrofiados. Nossos resultados sugerem que o desenvolvimento da fibrose intersticial e da hipertrofia dos cardiomiócitos pode ocorrer em momentos distintos, sendo que a avaliação conjunta do TVIMA e da FVEC pode acompanhar esses achados não invasivamente. A habilidade de seguir conjuntamente tanto a hipertrofia celular como a fibrose intersticial pode ser útil na avaliação do remodelamento miocárdico, especialmente quando se pretende avaliar o efeito de terapias anti-remodelamento.

Medidas de T1 após a administração de contraste tem sido utilizadas como um índice patológico de fibrose, em modelos animais (88,89) e em pacientes (90). A extensão dessa abordagem para investigar a hipertrofia dos cardiomiócitos nunca foi realizada com algum método não invasivo. Outro grupo, estudando pacientes com estenose aórtica, se interessou em desenvolver um método para avaliar o tamanho das células, porém com uma abordagem muito mais simplista e não direta, além de não ter sido realizado validação contra histologia (91). Nossos resultados sugerem que é possível medir longitudinalmente e de forma independente pela RMC a expansão da matriz extracelular e da hipertrofia celular.

Sabemos que o aumento da massa cardíaca pode resultar em expansão da matriz extracelular além de hipertrofia dos cardiomiócitos (14). A diferenciação entre a hipertrofia fisiológica e hipertrofia patológica pode necessitar mais informações do que apenas a massa ventricular e espessura das paredes do ventrículo esquerdo, tais como fibrose intersticial e tamanho dos cardiomiócitos. Na hipertrofia patológica, secundária à sobrecarga pressórica,

a hipertrofia celular pode ser considerada um marcador precoce de remodelamento miocárdico, ocorrendo antes da expansão da matriz celular e da disfunção ventricular esquerda e insuficiência cardíaca (13,78,79). Dados mostram que o estresse mecânico no músculo cardíaco é capaz de ativar fatores estimulantes da hipertrofia e fibrose, fatores estes envolvidos no desenvolvimento da insuficiência cardíaca (92-95). Dessa forma o aumento da fibrose intersticial parece ser um importante fator na transição da hipertrofia compensada e fisiológica para hipertrofia patológica e insuficiência cardíaca (78,96,97). Nos pacientes com HVE em risco para desenvolver insuficiência cardíaca, o equilíbrio no metabolismo do colágeno, identifica os pacientes em maior risco para apresenta insuficiência cardíaca clinica (98-100). Intervenção precoces, antes da ocorrência de fibrose intersticial e disfunção ventricular esquerda, pode ser útil na tentativa de evitara progressão para insuficiência cardíaca com sintomas (101).

O presente estudo apresenta algumas limitações: o uso da FVEC como um marcador de fibrose intersticial assume que a expansão do espaço extracelular ocorre de maneira homogenia pelo miocárdio. Outra limitação refere-se ao fato de não estarem disponíveis dados sobre a função diastólica nos experimentos com modelos animais, apenas na coorte de pacientes hipertensos. No caso dos camundongos, observamos associação significativa entre a FVEC e função sistólica do ventrículo esquerdo.

Nossa observação da subestimação da FVEC com o uso de modelo linear para análise dos dados das medidas de T1 pela RMC se aplica em situações que o R1 no plasma é relativamente elevado. Para R1 no plasma <2,0 segundos, a subestimação da determinação da FVEC foi relativamente pequena, da ordem de 5%. Dessa forma a comparação dos resultados da quantificação da FVEC depende da dose máxima do contraste gadolínio administrada.

Além disso, o presente estudo assume que permeabilidade da membrana celular dos cardiomiócitos é constante com o desenvolvimento da hipertrofia miocárdica. Apesar da isquemia poder alterar a permeabilidade da membrana celular (102), acreditamos que essa condição não está presente no nosso experimento pela ausência de RT pela RMC (102). A possível presença de outras células como os fibroblastos, pode introduzir potencial erro na determinação da hipertrofia de cardiomiócitos pelo nossa técnica. Apesar disso, o volume absoluto dessas outras células (não cardiomiócitos) é relativamente pequeno em comparação com o tamanho ocupado pelos cardiomiócitos.

5- CONCLUSÃO GERAL

A FVEC, quantificada por medidas de T1 derivadas da RMC, detectou a expansão de matriz extracelular, como um marcador de fibrose intersticial, em um modelo de doença cardíaca hipertensiva em camundongos e em uma coorte de pacientes hipertensos. A análise dos tempos de T1 com a prerrogativa da existência da troca de água pela membrana celular resulta em significativa subestimação da FVEC.

Nesse estudo validamos, utilizando dois modelos experimentais de sobrecarga pressórica no miocárdio, um método não invasivo, derivado de medidas de T1 pela RMC, para avaliação da hipertrofia dos cardiomiócitos e da expansão do espaço extracelular.

6- REFERÊNCIAS BIBLIOGRÁFICAS

1- Hill JA, Olson EN. Cardiac plasticity. N Engl J Med. [Research Support, N.I.H., Extramural Research Support, Non-U.S. Gov't Review]. 2008 Mar 27;358(13):1370-80.

2- Bernardo BC, Weeks KL, Pretorius L, McMullen JR. Molecular distinction between physiological and pathological cardiac hypertrophy: experimental findings and therapeutic strategies. Pharmacol Ther. [Research Support, Non-U.S. Gov't Review]. 2010 Oct;128(1):191-227.

3- de Simone G, Gottdiener JS, Chinali M, Maurer MS. Left ventricular mass predicts heart failure not related to previous myocardial infarction: the Cardiovascular Health Study. Eur Heart J. [Multicenter Study Research Support, N.I.H., Extramural]. 2008 Mar;29(6):741-7.

4- Krauser DG, Devereux RB. Ventricular hypertrophy and hypertension: prognostic elements and implications for management. Herz. [Comparative Study Review]. 2006 Jun;31(4):305-16.

5- Lip GY, Felmeden DC, Li-Saw-Hee FL, Beevers DG. Hypertensive heart disease. A complex syndrome or a hypertensive 'cardiomyopathy'? Eur Heart J. [Research Support, Non-U.S. Gov't Review]. 2000 Oct;21(20):1653-65.

6- Katz AM. Maladaptive growth in the failing heart: the cardiomyopathy of overload. Cardiovasc Drugs Ther. [Historical Article Review]. 2002 May;16(3):245-9.

7- Diamond JA, Phillips RA. Hypertensive heart disease. Hypertens Res. [Review]. 2005 Mar;28(3):191-202.

8- Diez J, Frohlich ED. A translational approach to hypertensive heart disease. Hypertension. [Research Support, Non-U.S. Gov't Review]. 2010 Jan;55(1):1-8.

9- Raman SV. The hypertensive heart. An integrated understanding informed by imaging. J Am Coll Cardiol. [Research Support, N.I.H., Extramural Review]. 2010 Jan 12;55(2):91-6.

10- Alpert NR, Mulieri LA. Increased myothermal economy of isometric force generation in compensated cardiac hypertrophy induced by pulmonary artery constriction in the rabbit. A characterization of heat liberation in normal and hypertrophied right ventricular papillary muscles. Circ Res. [Research Support, Non-U.S. Gov't Research Support, U.S. Gov't, P.H.S.]. 1982 Apr;50(4):491-500.

11- Frohlich ED, Gonzalez A, Diez J. Hypertensive left ventricular hypertrophy risk: beyond adaptive cardiomyocytic hypertrophy. J Hypertens. [Research Support, Non-U.S. Gov't Review]. 2011 Jan;29(1):17-26.

12- Agabiti-Rosei E, Muiesan ML, Salvetti M. Evaluation of subclinical target organ damage for risk assessment and treatment in the hypertensive patients: left ventricular hypertrophy. J Am Soc Nephrol. [Review]. 2006 Apr; 17(4 Suppl 2):S104-8.

13- Lorell BH, Carabello BA. Left ventricular hypertrophy: pathogenesis, detection, and prognosis. Circulation. [Review]. 2000 Jul 25;102(4):470-9.

14- Dorn GW, 2nd, Robbins J, Sugden PH. Phenotyping hypertrophy: eschew obfuscation. Circulation Research. [Editorial Historical Article Research Support, U.S. Gov't, P.H.S.]. 2003 Jun 13;92(11):1171-5.

15- Gradman AH, Alfayoumi F. From left ventricular hypertrophy to congestive heart failure: management of hypertensive heart disease. Prog Cardiovasc Dis. [Review]. 2006 Mar-Apr;48(5):326-41.

16- Weber KT, Brilla CG. Pathological hypertrophy and cardiac interstitium. Fibrosis and renin-angiotensin-aldosterone system. Circulation. [Research Support, U.S. Gov't, P.H.S. Review]. 1991 Jun;83(6):1849-65.

17- Opie LH, Commerford PJ, Gersh BJ, Pfeffer MA. Controversies in ventricular remodelling. Lancet. [Review]. 2006 Jan 28;367(9507):356-67.

18- Gaasch WH, Zile MR. Left ventricular structural remodeling in health and disease: with special emphasis on volume, mass, and geometry. Journal of the American College of Cardiology. [Review]. 2011 Oct 18;58(17):1733-40.

19- Verdecchia P, Angeli F, Achilli P, Castellani C, Broccatelli A, Gattobigio R, et al. Echocardiographic left ventricular hypertrophy in hypertension: marker for future events or mediator of events? Curr Opin Cardiol. [Research Support, Non-U.S. Gov't Review]. 2007 Jul;22(4):329-34.

20- Brunner-La Rocca HP. Do we understand why the heart fails? Eur Heart J. [Comment Editorial]. 2008 Mar;29(6):698-700.

21- Koren MJ, Devereux RB, Casale PN, Savage DD, Laragh JH. Relation of left ventricular mass and geometry to morbidity and mortality in uncomplicated essential hypertension. Ann Intern Med. [Research Support, U.S. Gov't, P.H.S.]. 1991 Mar 1;114(5):345-52.

22- Flint A. A practical treatise on the diagnosis, pathology, and treatment of diseases of the heart. 2d ed. Philadelphia, H. C. Lea; 1870.

23- Osler W. The principles and practice of medicine: designed for the use of practitioners and students of medicine. New York: D. Appleton and Company; 1892.

24- Izzo JL, Sica DA, Black HR. Council for High Blood Pressure Research (American Heart Association). Hypertension primer: [the essentials of high blood pressure: basic science, population science, and clinical management]. 4th ed. Philadelphia, PA: Lippincott Williams & Wilkins; 2008.

25- Devereux RB, Bella JN, Palmieri V, Oberman A, Kitzman DW, Hopkins PN, et al. Left ventricular systolic dysfunction in a biracial sample of hypertensive adults: The Hypertension Genetic Epidemiology Network (HyperGEN) Study. Hypertension. [Multicenter Study Research Support, U.S. Gov't, P.H.S.]. 2001 Sep;38(3):417-23.

26- Devereux RB, Roman MJ, Paranicas M, Lee ET, Welty TK, Fabsitz RR, et al. A population-based assessment of left ventricular systolic dysfunction in middle-aged and older adults: the Strong Heart Study. Am Heart J. [Research Support, U.S. Gov't, P.H.S.]. 2001 Mar;141(3):439-46.

27- Wachtell K, Rokkedal J, Bella JN, Aalto T, Dahlof B, Smith G, et al. Effect of electrocardiographic left ventricular hypertrophy on left ventricular systolic function in systemic hypertension (The LIFE Study). Losartan Intervention for Endpoint. Am J Cardiol. [Research Support, Non-U.S. Gov't Research Support, U.S. Gov't, P.H.S.]. 2001 Jan 1;87(1):54-60.

28- Arnold JM, Yusuf S, Young J, Mathew J, Johnstone D, Avezum A, et al. Prevention of Heart Failure in Patients in the Heart Outcomes Prevention Evaluation (HOPE) Study. Circulation. [Clinical Trial Multicenter Study Randomized Controlled Trial Research Support, Non-U.S. Gov't]. 2003 Mar 11;107(9):1284-90.

29- Perlini S, Muiesan ML, Cuspidi C, Sampieri L, Trimarco B, Aurigemma GP, et al. Midwall mechanics are improved after regression of hypertensive left ventricular hypertrophy and normalization of chamber geometry. Circulation 2001 Feb 6;103(5):678-83.

30- Wachtell K, Palmieri V, Olsen MH, Gerdts E, Papademetriou V, Nieminen MS, et al. Change in systolic left ventricular performance after 3 years of antihypertensive treatment: the Losartan Intervention for Endpoint (LIFE) Study. Circulation. [Clinical Trial Multicenter Study Randomized Controlled Trial Research Support, Non-U.S. Gov't]. 2002 Jul 9;106(2):227-32.

31- Susic D, Frohlich ED. Optimal treatment of hypertension with diastolic heart failure. Heart Fail Clin. [Review]. 2008 Jan;4(1):117-24.

32- Devereux RB, Roman MJ, Liu JE, Welty TK, Lee ET, Rodeheffer R, et al. Congestive heart failure despite normal left ventricular systolic function in a population-based sample: the Strong Heart Study. Am J Cardiol. [Research Support, U.S. Gov't, P.H.S.]. 2000 Nov 15;86(10):1090-6.

33- Kannel WB, Levy D, Cupples LA. Left ventricular hypertrophy and risk of cardiac failure: insights from the Framingham Study. J Cardiovasc Pharmacol. [Research Support, Non-U.S. Gov't Research Support, U.S. Gov't, P.H.S.]. 1987;10 Suppl 6:S135-40.

34- Swynghedauw B, Delcayre C, Samuel JL, Mebazaa A, Cohen-Solal A. Molecular mechanisms in evolutionary cardiology failure. Ann N Y Acad Sci. [Review]. 2010 Feb;1188:58-67.

35- Samuel JL, Swynghedauw B. Is cardiac hypertrophy a required compensatory mechanism in pressure-overloaded heart? J Hypertens. [Comment Editorial]. 2008 May;26(5):857-8.

36- Buckberg GD, Coghlan HC, Hoffman JI, Torrent-Guasp F. The structure and function of the helical heart and its buttress wrapping. VII. Critical importance of septum for right ventricular function. Semin Thorac Cardiovasc Surg. [Review]. 2001 Oct;13(4):402-16.

37- Feihl F, Liaudet L, Waeber B. The macrocirculation and microcirculation of hypertension. Curr Hypertens Rep. [Review]. 2009 Jun;11(3):182-9.

38- Lapu-Bula R, Ofili E. From hypertension to heart failure: role of nitric oxide-mediated endothelial dysfunction and emerging insights from myocardial contrast echocardiography. Am J Cardiol. [Research Support, N.I.H., Extramural Research Support, U.S. Gov't, Non-P.H.S. Review]. 2007 Mar 26;99(6B):7D-14D.

39- London GM, Guerin AP. Influence of arterial pulse and reflected waves on blood pressure and cardiac function. Am Heart J. [Review]. 1999 Sep; 138(3 Pt 2):220-4.

40- Weber KT. Fibrosis and hypertensive heart disease. Curr Opin Cardiol. [Review]. 2000 Jul;15(4):264-72.

41- Burlew BS, Weber KT. Cardiac fibrosis as a cause of diastolic dysfunction. Herz. [Review]. 2002 Mar;27(2):92-8.

42- McLenachan JM, Dargie HJ. Ventricular arrhythmias in hypertensive left ventricular hypertrophy. Relationship to coronary artery disease, left ventricular dysfunction, and myocardial fibrosis. Am J Hypertens. [Research Support, Non-U.S. Gov't]. 1990 Oct;3(10):735-40.

43- McLenachan JM, Henderson E, Morris KI, Dargie HJ. Ventricular arrhythmias in patients with hypertensive left ventricular hypertrophy. N Engl J Med. [Research Support, Non-U.S. Gov't]. 1987 Sep 24;317(13):787-92.

44- Frohlich ED. Fibrosis and ischemia: the real risks in hypertensive heart disease. Am J Hypertens. [Review]. 2001 Jun;14(6 Pt 2):194S-9S.

45- Khan R, Sheppard R. Fibrosis in heart disease: understanding the role of transforming growth factor-beta in cardiomyopathy, valvular disease and arrhythmia. Immunology. [Review]. 2006 May;118(1):10-24.

46- Young MJ. Mechanisms of mineralocorticoid receptor-mediated cardiac fibrosis and vascular inflammation. Curr Opin Nephrol Hypertens. [Review]. 2008 Mar;17(2):174-80.

47- Gonzalez A, Lopez B, Ravassa S, Querejeta R, Larman M, Diez J, et al. Stimulation of cardiac apoptosis in essential hypertension: potential role of angiotensin II. Hypertension. [Clinical Trial Randomized Controlled Trial Research Support, Non-U.S. Gov't]. 2002 Jan;39(1):75-80.

48- Yamamoto S, Sawada K, Shimomura H, Kawamura K, James TN. On the nature of cell death during remodeling of hypertrophied human myocardium. J Mol Cell Cardiol. [Research Support, Non-U.S. Gov't]. 2000 Jan;32(1):161-75.

49- Ravassa S, Gonzalez A, Lopez B, Beaumont J, Querejeta R, Larman M, et al. Upregulation of myocardial Annexin A5 in hypertensive heart disease: association with systolic dysfunction. Eur Heart J. [Research Support, Non-U.S. Gov't]. 2007 Nov;28(22):2785-91.

50- Narula J, Arbustini E, Chandrashekhar Y, Schwaiger M. Apoptosis and the systolic dysfunction in congestive heart failure. Story of apoptosis interruptus and zombie myocytes. Cardiol Clin. [Review]. 2001 Feb;19(1):113-26.

51- Bleeker GB, Bax JJ, Steendijk P, Schalij MJ, van der Wall EE. Left ventricular dyssynchrony in patients with heart failure: pathophysiology, diagnosis and treatment. Nat Clin Pract Cardiovasc Med. [Comparative Study Review]. 2006 Apr;3(4):213-9.

52- Spragg DD, Kass DA. Pathobiology of left ventricular dyssynchrony and resynchronization. Prog Cardiovasc Dis. [Review]. 2006 Jul-Aug;49(1):26-41.

53- Kim RJ, Wu E, Rafael A, Chen EL, Parker MA, Simonetti O, et al. The use of contrast-enhanced magnetic resonance imaging to identify reversible myocardial dysfunction. NEnglJMed 2000;343(20):1445-53.

54- Kim RJ, Fieno DS, Parrish TB, Harris K, Chen EL, Simonetti O, et al. Relationship of MRI delayed contrast enhancement to irreversible injury, infarct age, and contractile function. Circulation1999 Nov 9;100(19):1992-2002.

55- Tandri H, Saranathan M, Rodriguez ER, Martinez C, Bomma C, Nasir K, et al. Noninvasive detection of myocardial fibrosis in arrhythmogenic right ventricular cardiomyopathy using delayed-enhancement magnetic resonance imaging. J Am Coll Cardiol 2005 Jan 4;45(1):98-103.

56- Hunold P, Wieneke H, Bruder O, Krueger U, Schlosser T, Erbel R, et al. Late enhancement: a new feature in MRI of arrhythmogenic right ventricular cardiomyopathy? J Cardiovasc Magn Reson 2005;7(4):649-55.

57- Harris PA, Lorenz CH, Holburn GE, Overholser KA. Regional measurement of the Gd-DTPA tissue partition coefficient in canine myocardium. Magn Reson Med 1997 Oct;38(4):541-5.

58- Flacke SJ, Fischer SE, Lorenz CH. Measurement of the gadopentetate dimeglumine partition coefficient in human myocardium in vivo: normal distribution and elevation in acute and chronic infarction. Radiology 2001 Mar;218(3):703-10.

59- Elliott P. Pathogenesis of cardiotoxicity induced by anthracyclines. Semin Oncol 2006 Jun;33(3 Suppl 8):S2-7.

60- Iles L, Pfluger H, Phrommintikul A, Cherayath J, Aksit P, Gupta SN, et al. Evaluation of diffuse myocardial fibrosis in heart failure with cardiac magnetic resonance contrast-enhanced T1 mapping. J Am Coll Cardiol 2008 Nov 4;52(19):1574-80.

61- Ellinor PT, Sasse-Klaassen S, Probst S, Gerull B, Shin JT, Toeppel A, et al. A novel locus for dilated cardiomyopathy, diffuse myocardial fibrosis, and sudden death on chromosome 10q25-26. J Am Coll Cardiol 2006 Jul 4;48(1):106-11.

62- Kehr E, Sono M, Chugh SS, Jerosch-Herold M. Gadolinium-enhanced magnetic resonance imaging for detection and quantification of fibrosis in human myocardium in vitro. Int J Cardiovasc Imaging 2008 Jan;24(1):61-8.

63- Flett AS, Hayward MP, Ashworth MT, Hansen MS, Taylor AM, Elliott PM, et al. Equilibrium contrast cardiovascular magnetic resonance for the measurement of diffuse myocardial fibrosis: preliminary validation in humans. Circulation Jul 13;122(2):138-44.

64- Mongeon FP, Jerosch-Herold M, Coelho-Filho OR, Blankstein R, Falk RH, Kwong RY. Quantification of extracellular matrix expansion by CMR in infiltrative heart disease. JACC Cardiovasc Imaging. [Research Support, N.I.H., Extramural Research Support, Non-U.S. Gov't]. 2012 Sep;5(9):897-907.

65- Neilan TG, Coelho-Filho OR, Shah RV, Feng JH, Pena-Herrera D, Mandry D, et al. Myocardial Extracellular Volume by Cardiac Magnetic Resonance Imaging in Patients Treated With Anthracycline-Based Chemotherapy. Am J Cardiol 2012 Dec 7.

66- Jerosch-Herold M, Sheridan DC, Kushner JD, Nauman D, Burgess D, Dutton D, et al. Cardiac magnetic resonance imaging of myocardial contrast uptake and blood flow in patients affected with idiopathic or familial dilated cardiomyopathy. Am J Physiol 2008 Sep;295(3):H1234-H42.

67- Han Y, Peters DC, Dokhan B, Manning WJ. Shorter difference between myocardium and blood optimal inversion time suggests diffuse fibrosis in dilated cardiomyopathy. J Magn Reson Imaging 2009 Nov;30(5):967-72.

68- Han Y, Peters D, Manning W. Diffuse fibrosis in dilated cardiomyopathy results in a shorter myocardial null time. Journal of Cardiovascular Magnetic Resonance 2009;11(Suppl 1):P286.

69- Friedrich MG. There is more than shape and function. J Am Coll Cardiol 2008 Nov 4;52(19):1581-3.

70- Flett AS, Hayward MP, Ashworth MT, Hansen MS, Taylor AM, Elliott PM, et al. Equilibrium contrast cardiovascular magnetic resonance for the measurement of diffuse myocardial fibrosis: preliminary validation in humans. Circulation 2010 Jul 13;122(2):138-44.

71- Thornhill RE, Prato FS, Wisenberg G, White JA, Nowell J, Sauer A. Feasibility of the single-bolus strategy for measuring the partition coefficient of Gd-DTPA in patients with myocardial infarction: independence of image delay time and maturity of scar. Magn Reson Med 2006 Apr;55(4):780-9.

72- Pereira RS, Prato FS, Wisenberg G, Sykes J. The determination of myocardial viability using Gd-DTPA in a canine model of acute myocardial ischemia and reperfusion. Magn Reson Med 1996;36(5):684-93.

73- Lekx KS, Prato FS, Sykes J, Wisenberg G. The partition coefficient of Gd-DTPA reflects maintained tissue viability in a canine model of chronic significant coronary stenosis. J Cardiovasc Magn Reson 2004;6(1):33-42.

74- Anversa P, Hiler B, Ricci R, Guideri G, Olivetti G. Myocyte cell loss and myocyte hypertrophy in the aging rat heart. J Am Coll Cardiol. [Research Support, Non-U.S. Gov't Research Support, U.S. Gov't, P.H.S.]. 1986 Dec;8(6):1441-8.

75- Kajstura J, Zhang X, Reiss K, Szoke E, Li P, Lagrasta C, et al. Myocyte cellular hyperplasia and myocyte cellular hypertrophy contribute to chronic ventricular remodeling in coronary artery narrowing-induced cardiomyopathy in rats. Circ Res. [Research Support, U.S. Gov't, P.H.S.]. 1994 Mar;74(3):383-400.

76- Landis CS, Li X, Telang FW, Molina PE, Palyka I, Vetek G, et al. Equilibrium transcytolemmal water-exchange kinetics in skeletal muscle in vivo. Magnetic resonance in medicine: official journal of the Society of Magnetic Resonance in Medicine / Society of Magnetic Resonance in Medicine. [Research Support, U.S. Gov't, Non-P.H.S. Research Support, U.S. Gov't, P.H.S.]. 1999 Sep;42(3):467-78.

77- Pais A. "Subtle is the Lord-- ": the science and the life of Albert Einstein. Oxford Oxfordshire ; New York: Oxford University Press; 1982.

78- Boluyt MO, O'Neill L, Meredith AL, Bing OH, Brooks WW, Conrad CH, et al. Alterations in cardiac gene expression during the transition from stable hypertrophy to heart failure. Marked upregulation of genes encoding extracellular matrix components. Circulation Research. [Research Support, Non-U.S. Gov't Research Support, U.S. Gov't, Non-P.H.S.]. 1994 Jul;75(1):23-32.

79- Scimia MC, Hurtado C, Ray S, Metzler S, Wei K, Wang J, et al. APJ acts as a dual receptor in cardiac hypertrophy. Nature2012 Jul 18.

80- Xu J, Kimball TR, Lorenz JN, Brown DA, Bauskin AR, Klevitsky R, et al. GDF15/MIC-1 functions as a protective and antihypertrophic factor released from the myocardium in association with SMAD protein activation. Circ Res 2006 Feb 17;98(3):342-50.

81- Landis CS, Li X, Telang FW, Coderre JA, Micca PL, Rooney WD, et al. Determination of the MRI contrast agent concentration time course in vivo following bolus injection: effect of equilibrium transcytolemmal water exchange. Magn Reson Med 2000 Oct;44(4):563-74.

82- Litwin SE, Katz SE, Morgan JP, Douglas PS. Long-term captopril treatment improves diastolic filling more than systolic performance in rats with large myocardial infarction. J Am Coll Cardiol. [Research Support, Non-U.S. Gov't Research Support, U.S. Gov't, Non-P.H.S. Research Support, U.S. Gov't, P.H.S.]. 1996 Sep;28(3):773-81.

83- Bench T, Burkhoff D, O'Connell JB, Costanzo MR, Abraham WT, St John Sutton M, et al. Heart failure with normal ejection fraction: consideration of mechanisms other than diastolic dysfunction. Curr Heart Fail Rep. [Review]. 2009 Mar;6(1):57-64.

84- Litwin SE, Grossman W. Diastolic dysfunction as a cause of heart failure. J Am Coll Cardiol. [Research Support, U.S. Gov't, P.H.S. Review]. 1993 Oct; 22(4 Suppl A):49A-55A.

85- Swartz MF, Fink GW, Sarwar MF, Hicks GL, Yu Y, Hu R, et al. Elevated pre-operative serum peptides for collagen I and III synthesis result in post-surgical atrial fibrillation. J Am Coll Cardiol. [Research Support, N.I.H., Extramural Research Support, Non-U.S. Gov't]. 2012 Oct 30;60(18):1799-806.

86- Landis CS, Li X, Telang FW, Coderre JA, Micca PL, Rooney WD, et al. Determination of the MRI contrast agent concentration time course in vivo following bolus injection: effect of equilibrium transcytolemmal water exchange. Magnetic resonance in medicine: official journal of the Society of Magnetic Resonance in Medicine / Society of Magnetic Resonance in Medicine. [Research Support, U.S. Gov't, Non-P.H.S. Research Support, U.S. Gov't, P.H.S.]. 2000 Oct;44(4):563-74.

87- Artham SM, Lavie CJ, Milani RV, Patel DA, Verma A, Ventura HO. Clinical impact of left ventricular hypertrophy and implications for regression. Prog Cardiovasc Dis. [Review]. 2009 Sep-Oct;52(2):153-67.

88- Messroghli DR, Nordmeyer S, Buehrer M, Kozerke S, Dietrich T, Kaschina E, et al. Small animal Look-Locker inversion recovery (SALLI) for simultaneous generation of cardiac T1 maps and cine and inversion recovery-prepared images at high heart rates: initial experience. Radiology 2011 Oct;261(1):258-65.

89- Messroghli DR, Nordmeyer S, Dietrich T, Dirsch O, Kaschina E, Savvatis K, et al. Assessment of diffuse myocardial fibrosis in rats using small-animal Look-Locker inversion recovery T1 mapping. Circ Cardiovasc Imaging. [Comparative Study Research Support, Non-U.S. Gov't]. 2011 Nov;4(6):636-40.

90- Ugander M, Oki AJ, Hsu LY, Kellman P, Greiser A, Aletras AH, et al. Extracellular volume imaging by magnetic resonance imaging provides insights into overt and sub-clinical myocardial pathology. Eur Heart J. [Research Support, N.I.H., Intramural]. 2012 May;33(10):1268-78.

91- Neilan TG, Coelho-Filho OR, Pena-Herrera D, Shah RV, Jerosch-Herold M, Francis SA, et al. Left ventricular mass in patients with a cardiomyopathy after treatment with anthracyclines. Am J Cardiol. [Comparative Study Research Support, N.I.H., Extramural Research Support, Non-U.S. Gov't]. 2012 Dec 1;110(11):1679-86.

92- Adams JW, Sakata Y, Davis MG, Sah VP, Wang Y, Liggett SB, et al. Enhanced Galphaq signaling: a common pathway mediates cardiac hypertrophy and apoptotic heart failure. Proceedings of the National Academy of Sciences of the United States of America. [Research Support, Non-U.S. Gov't Research Support, U.S. Gov't, Non-P.H.S. Research Support, U.S. Gov't, P.H.S.]. 1998 Aug 18;95(17):10140-5.

93- Hein S, Arnon E, Kostin S, Schonburg M, Elsasser A, Polyakova V, et al. Progression from compensated hypertrophy to failure in the pressure-overloaded human heart: structural deterioration and compensatory mechanisms. Circulation 2003 Feb 25;107(7):984-91.

94- Krayenbuehl HP, Hess OM, Monrad ES, Schneider J, Mall G, Turina M. Left ventricular myocardial structure in aortic valve disease before, intermediate, and late after aortic valve replacement. Circulation. [Comparative Study Research Support, Non-U.S. Gov't]. 1989 Apr;79(4):744-55.

95- Sanada S, Hakuno D, Higgins LJ, Schreiter ER, McKenzie AN, Lee RT. IL-33 and ST2 comprise a critical biomechanically induced and cardioprotective signaling system. The Journal of Clinical Investigation. [Research Support, N.I.H., Extramural Research Support, Non-U.S. Gov't]. 2007 Jun;117(6):1538-49.

96- Mohammed SF, Ohtani T, Korinek J, Lam CS, Larsen K, Simari RD, et al. Mineralocorticoid accelerates transition to heart failure with preserved ejection fraction via "nongenomic effects". Circulation. [Research Support, N.I.H., Extramural Research Support, Non-U.S. Gov't]. 2010 Jul 27;122(4):370-8.

97- Shapiro BP, Owan TE, Mohammed S, Kruger M, Linke WA, Burnett JC, Jr., et al. Mineralocorticoid signaling in transition to heart failure with normal ejection fraction. Hypertension. [Research Support, N.I.H., Extramural Research Support, Non-U.S. Gov't]. 2008 Feb;51(2):289-95.

98- Ahmed SH, Clark LL, Pennington WR, Webb CS, Bonnema DD, Leonardi AH, et al. Matrix metalloproteinases/tissue inhibitors of metalloproteinases: relationship between changes in proteolytic determinants of matrix composition and structural, functional, and clinical manifestations of hypertensive heart disease. Circulation. [Research Support, N.I.H., Extramural Research Support, Non-U.S. Gov't Research Support, U.S. Gov't, Non-P.H.S.]. 2006 May 2;113(17):2089-96.

99- Martos R, Baugh J, Ledwidge M, O'Loughlin C, Murphy NF, Conlon C, et al. Diagnosis of heart failure with preserved ejection fraction: improved accuracy with the use of markers of collagen turnover. European Journal of Heart Failure 2009 Feb;11(2):191-7.

100- Post WS, Larson MG, Myers RH, Galderisi M, Levy D. Heritability of left ventricular mass: the Framingham Heart Study. Hypertension 1997 Nov;30(5):1025-8.

101- Sorenson AL, Tepper D, Sonnenblick EH, Robinson TF, Capasso JM. Size and shape of enzymatically isolated ventricular myocytes from rats and cardiomyopathic hamsters. Cardiovasc Res 1985 Dec;19(12):793-9.

102- Boyett MR, Frampton JE, Kirby MS. The length, width and volume of isolated rat and ferret ventricular myocytes during twitch contractions and changes in osmotic strength. Exp Physiol 1991 Mar;76(2):259-70.